MARMARA UNIVERSITY
INSTITUTE FOR GRADUATE STUDIES
IN PURE AND APPLIED SCIENCES

Design and Analysis of Automated Storage and Retrieval System Mast

Ozan Erdem Demirel

MASTER THESIS

Department of Mechanical Engineering

Thesis Supervisor

Assoc. Prof. IBRAHIM SINA KUSEYRI

ISTANBUL, 2022

MARMARA UNIVERSITY
INSTITUTE FOR GRADUATE STUDIES
IN PURE AND APPLIED SCIENCES

Design and Analysis of Automated Storage and Retrieval System Mast

Ozan Erdem Demirel
Student no: o524620008

MASTER THESIS
Department of Mechanical Engineering

Thesis Supervisor
Assoc. Prof. IBRAHIM SINA KUSEYRI

ISTANBUL, 2022

MARMARA UNIVERSITY
INSTITUTE FOR GRADUATE STUDIES IN PURE AND APPLIED SCIENCES

Ozan Erdem Demirel, a Master of Science student of Marmara University Institute for Graduate Studies in Pure and Applied Sciences, defended his thesis entitled "Design and Analysis of Automated Storage and Retrieval System Mast", on July 4, 2022 and has been found to be satisfactory by the jury members.

Jury Members

Doç. Dr. İbrahim Sina Kuseyri (Advisor)
Marmara University .....(SIGN).....

Doç. Dr. Mehmet Berke Gür (Jury)
Bahçeşehir University .....(SIGN).....

Dr. Öğr. Üyesi Uğur Tümerdem (Jury)
Marmara University .....(SIGN).....

APPROVAL

Marmara University Institute for Graduate Studies in Pure and Applied Sciences Executive Committee approves that Ozan Erdem DEMIREL be granted the degree of Master of Science in Department of Mechanical Engineering, Mechanical Engineering Master Program on ..... . (Resolution no:).

Director of the Institute
Prof. Dr. Bülent Ekici

ACKNOWLEDGEMENT

I would like to thank my thesis Advisor Assoc. Prof. İbrahim Sina KUSEYRI for taking the time to help me out through this thesis.

During the entire period of my master's degree, Altınay Robot Technologies and especially my leader Ali KAYA had always supported me to taking the time I need for my courses, writing the thesis and other miscellaneous times.

I wouldn't have completed my graduate education without the help of my friends who always support me through the hard times. Ahmet Semih PARLAK had always act like a mentor, gave me the mindset how to make a research and the resilience to complete my master's degree. My colleagues Furkan Ermanas YABANCI, Betül YURDDAŞ and Ayten BİNAY always helped me during hard times, not only for work, also with emotional support.

Last and most importantly I present my deepest gratefulness to my mother Yeşim ERDEM and father İlhan DEMİREL, for supporting me and my decisions and providing me all the tools and support that I need to complete my educations.

June 2022

Ozan Erdem Demirel

(Mechanical Engineer)

Contents

ÖZET iv

ABSTRACT v

SYMBOLS vi

ABBREVIATIONS vii

LIST OF FIGURES viii

LIST OF TABLES xi

1 INTRODUCTION 1

1.1 Types of Automated Storage Retrieval Systems 3

1.2 Stacker Crane Structure 5

1.3 Literature Survey 7

1.4 Motivation and Objective 9

2 Stacker Crane Design 9

2.1 Mast Construction Determination 11

2.2 Stacker Crane Parameters 14

2.2.1 Lateral Stiffness of The Double Mast Stacker Crane 14

2.3 Finite Element Analysis of the Mast 18

2.4 Dynamic Analysis of the Structure 22

2.4.1 Wheel Loads 27

2.5 Motor Selection and Cycle Calculation 28

2.5.1 RMS Torque Calculation 30

2.5.1.1 RMS Torque calculation for X axis . . . 31
2.5.1.2 RMS Torque calculation for Y axis . . . 38
2.6 Safety Equipment and Sensors 42

3 Control of Stacker Crane **44**
3.1 Mathematical Model Derivation 45
3.2 Natural Frequency of Stacker Crane 46
3.3 State Space Representation of the Stacker Crane 47
3.4 Trajectory Planning 48
3.5 Feed-Forward Force Calculation 51
3.6 Control Approach 53
3.7 Notch Filter Design 57

4 Simulation Results **60**

5 Conclusion **62**
REFERENCES 63

ÖZET

OTOMATIK DEPOLAMA SISTEMI KULESININ TASARIMI VE KONTROLÜ

Depolama sistemlerinde; ürünlerin teslim alınması, yerleştirilmesi, sayımı, toplaması, kontrolü ve gönderilmesi gibi adımlar yer almaktadır. Otomatik depolama sistemleri sayesinde depolarda harcanan ölü alanlar azaltılmakta ve standart forklift sistemlerinin ulaşamayacağı yüksekliklerde yüksek kapasiteli depolama yapılabilmektedir. Standart depolarda istenilen yüksek taşıma kapasiteleri $(+500kg)$, hızlar $(+4m/s)$ ve ivmelenmeler $(+2m/s^2)$ sebebiyle robotik sistemlerde oldukça yüksek dinamik yükler ortaya çıkmaktadır. Yatırım maliyetleri sebebiyle sistemlerin ağırlığının düşürülmesi göz önünde bulundurulduğunda robotik sistemin kule tasarımında katılığının (rijitlik, stiffness) azalmasıyla durumuyla karşılaşılmakta ve bu sebeple sistemde yüksek titreşimlere sebep olmaktadır. Yapılan çalışmada otomatik depolama sisteminde kullanılan kule üzerine yoğunlaşılmış ve yapının tasarım ve analizi yapılmıştır. Basit mesnet olarak modellenen kule tasarımında; tasarım isterleri dahilinde, rijitlik, ağırlık ve boyut gibi parametrelerin optimizasyonunun yapılması hedeflenmektedir. Yapılan tasarımda dinamik kuvvetler, depolama kulesi yapısının incelenmesi, sistemin matematik modelinin çıkarılması, kontrol algoritmasının oluşturulması konuları ile tasarım tamamlanmıştır. Sonuç olarak bir otomatik depolama sisteminde kullanılan robotik sistemin tasarımı ile ilgili parametreler değerlendirilmiş ve titreşim kontrolünün yapılmasıyla sisteminin hızının optimal şekilde kullanılmasına ulaşılmıştır.

ABSTRACT

DESIGN AND ANALYSIS OF AUTOMATED STORAGE AND RETRIEVAL SYSTEM MAST

In automated storage systems, there are steps such as receiving, placing, counting, collecting, controlling, and sending the products. Thanks to automatic storage systems, dead spaces in warehouses are reduced, operator errors can be prevented, and high-capacity storage can be made at heights that standard forklift systems cannot reach. Established warehouses can be designed in various configurations according to the number of hourly product transfers expected from the system, and appropriate robotic systems are integrated into the system accordingly. Due to the high carrying capacities (+500kg), speeds (+4 m/s) and accelerations $(+2m/s^2)$ required in standard warehouses, very high dynamic loads arise in robotic systems. Considering the investment costs, it is quite normal to want to reduce the weight of every robotic system. Considering the same situation in these systems, the robotic system is faced with a decrease in the stiffness (rigidity) in the tower design, and therefore it causes high vibrations and wobbles in the system. In the work to be done, the tower used in the automatic storage system was focused on and the design and analysis of the structure was made. In the tower design modelled as a simple support; It is aimed to optimize parameters such as stiffness, weight, and size within the design requirements. The design was completed with dynamic forces, examination of the storage tower structure, mathematical modelling of the system, and creation of the control algorithm. As a result, parameters related to the design of the robotic system used in an automatic storage system were evaluated and an optimal evaluation of the speed of the system was achieved by performing vibration control.

SYMBOLS

E	: Modulus of elasticity
I	: Moment of inertia of a cross section
g	: Gravitational constant
η	: Efficiency
RPM	: Rotational speed per minute

ABBREVIATIONS

ASRS	:Automated storage and retrieval system
LHD	:Load handling device
FEA	:Finite element analysis
μ_k	:Static friction coefficient
RMS	:Root mean squared
PLC	:Programmable logic controller
FEA	:Finite element analysis
FOC	:Field-Oriented Control

LIST OF FIGURES

1.1 First ASRS concept, founded by Demag [20] 1

1.2 Productivity chart of a worker 2

1.3 Carousel type ASRS modules [19] 4

1.4 Stacker crane (Mecalux) [14] 5

1.5 Robotics based ASRS 5

1.6 Stacker crane components 6

2.1 Stacker crane payload configurations 10

2.2 Stacker crane racking configurations 11

2.3 Stacker Crane and Inverted Pendulum 11

2.4 Deflection of a simply supported beam 12

2.5 Rose+Kriger D-80x240 Aluminium Sigma Profile 14

2.6 Deformation of Double Mast Stacker Crane 15

2.7 Left: Isometric view Right:Dimensions of Stacker Crane . 15

2.8 Assumed model of stacker crane 17

2.9 Resultant moment and constraint forces on beams 19

2.10 Right angle connector [9] 20

2.11 1st resonance mode of stacker crane structure 21

2.12 2nd and 3rd resonance mode of stacker crane structure . . . 22

2.13 Drive configuration of mias miniload stacker crane [15] . 23

2.14 Dimensions of stacker crane according to center of mass . 24

2.15 Wheels of stacker crane [28] 28

2.16 Typical torque diagram for hoist across one conveying cycle [22] 30
2.17 Different command cycles of the stacker crane [27] 30
2.18 X axis drive-train 32
2.19 Trapezoidal motion profile [29] 35
2.20 X axis motor load diagram [24] 38
2.21 X axis motor graph [24] 38
2.22 Y axis drive-train 39
2.23 Y axis motor load diagram [24] 41
2.24 Y axis motor graph [24] 42
2.25 Safety Equipments 43
2.26 Miscellaneous Sensors 44

3.1 Motion system of the stacker crane with equivalent mass and spring 45
3.2 Trajectory profiles for 4th order system 50
3.3 Feed-Forward force block diagram 53
3.4 Control flow schematic 54
3.5 Induction motor simulink model 55
3.6 Profile Generator Block [10] 56
3.7 Stacker crane simulink model 57
3.8 Bode plot of the notch filter 58
3.9 Notch filter test in simulink 59
3.10 System response of the upper system in figure 3.9 with notch filter 59

3.11 System response of the lower system in figure 3.9 without notch filter 60

4.1 LHD parameters for sample trajectory 61

4.2 Trajectory follow error with and without feed-forward force 61

LIST OF TABLES

List of Tables

2.1 Parameters of mast profile 13

2.2 Parameters of stacker crane 14

2.3 FEA results 19

2.4 Dimensions of center of mass and load carrying wheels . . 26

2.5 Rolling friction of different materials [3] 34

2.6 Segment times for a cycle 36

2.7 X axis Motor load parameters by segments 37

2.8 Segment times for a cycle for y axis 40

2.9 Y Axis motor load parameters by segments 41

3.1 Bounds on parameters for sample trajectory 49

1. INTRODUCTION

Automated Storage and Retrieval Systems has been in the industry for a long time. It is now a key system for warehouses to automate their intralogistics. The technology as we use today was first developed in 1950s by Demag which is predecessor of Dematic.The first ASRS went into operation in 1962 in a book club in Germany, Gütersloh.[1]

The timing of this innovation could not be better with the rapidly growing supply chain operations. Also with the second industrial revolution, ASRS systems began to find a very large place in the market. With the computer and IT technologies expanded in 1980s and 1990s, sensors, magnets and control techniques were integrated in the system and helped position the machine more precisely. Meaning the pallets, boxes and other goods can be positioned in rack system safely.



Figure 1.1: First ASRS concept, founded by Demag [20]

In 1980 first computer controlled ASRS with three-dimensional warehouse was developed by China's Ministry of Machinery. Wide usage was first started in the state owned enterprises such as tobacco and medicine.

The importance of asrs systems is increasing day by day and as of 2019,

the market size has reached 7.6 $. The market size of the system certainly will grow as time goes on with the developments like; energy efficiency, weight reduction with state of the art construction materials, reduction in vibration of the mast with modern control solutions and dampening systems and increased lifespan.

ASRS solutions are used in variety of applications, some of which are;

- Goods to person order picking: The most time consuming task in the picking, packing and processing is the time to person to reach the item of interest. With using ASRS worker does not physically move, the item comes to the station instead. Once the requested item quantity picked, the stock returns to the storage and the next item fed to the station. Thus the worker effort utilized fully.

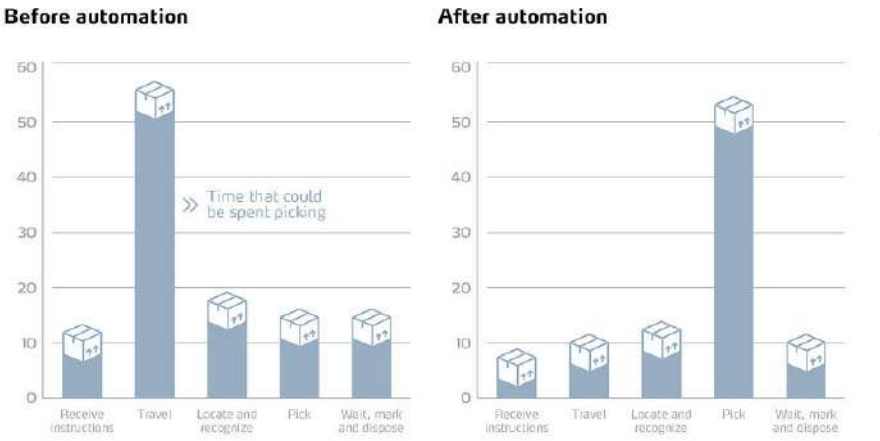

Figure 1.2: Productivity chart of a worker

- Stocking orders for shipping: Orders can be stocked in a designated area even without the employees are not being on the spot. This allows a certain amount of product can be placed in an area that later on a worker can collect goods all together.

- Point of use storage: Only way to respond advancing complex storage techniques, is to have a storage that it can be programmed or designed to requirements. By integrating ASRS with software such

as warehouse management systems (WMS); storage capacity can be fully utilized, data of the items can be tracked down and most sophisticated storage algorithms could be used.

With the usage of ASRS, many advancements in intralogistics can be obtainable. ASRS technologies offer high density storage with using modern machines in a compact footprint in such a way nearly most of the height of the warehouse could be used. Improved pick accuracy can be accomplished with worker friendly systems integrated with transport machines such as light directed picking technologies. Greater inventory control is possible with integration with warehouse management systems.

In the light of the facts stated; ASRS has become a must in modern intralogistics. Also with these systems getting easier to access, there is no doubt we all see them in our everyday locations such as pharmacies and libraries.

1.1 Types of Automated Storage Retrieval Systems

There are several types of ASRS machines which has a common main goal to basically transport a unit load a place to another. Solutions are different through the market, the selection process of the solution depends on the volume and type of the product and required speed (Goods per unit time) of the process. ASRS technologies can be separated into three main categories which are; shelf based picking, bin based picking and robotic picking. Countless machinery can be developed in these categories with changing speeds, different carrying capacities and volumes but the main working principle remains the same in a category. Several main machinery can be described as below;

- Vertical and Horizontal carousel modules;

Vertical carousel modules lets the user use overhead space effectively and horizontal modules are simple rotating carriage of bins. Products can be stored in predetermined shelves or in a tote on the shelves. Item volumes and weight are smaller comparing to other ASRS's. Items generally could be carried by the worker waiting at the pick & place area. Somebody can see this type of system in a home improvement store as they use this system to store carpets, vinyls and other large rolled goods.



(a) Vertical carousel

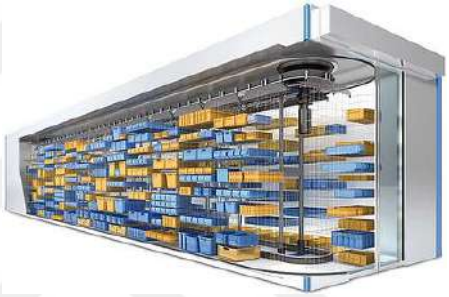

(b) Horizontal carousel

Figure 1.3: Carousel type ASRS modules [19]

- Crane based ASRS;

  System based on a automated crane in a central aisle and shelves on each side. Crane is used for to deliver the goods from shelves to conveyor system. Machinery could be designed to handle mini loads (from 50 to 100 kg) up to pallets reaching 1500kg weight. Companies generally has several types of stacker cranes that are designed beforehand and they suit the system according to customer requirements. Storage configuration on the shelves can be designed as single, double and multiple depth. Each aisle usually consist of a single stacker crane but it can be increased. There are also types that can change the aisle for servicing multiple shelves.

- Robotic based ASRS;



Figure 1.4: Stacker crane (Mecalux) [14]

Storage system solutions are endless. With state of the art robotic mechanisms, there is a new ASRS solution emerges. Dynamic storage algorithms, require sophisticated solutions which can be addressed by different types of robotic systems. Nowadays there are storage consist of mobile robots moving on top of the cubic storage and picks underneath the system, mobile floor robots that can navigate on storage floor without any guidance or a shuttle robot system that runs on a rack structure to store and retrieve goods.



(a) Cubic robotic storage



(b) Mobile robot (Amazon fulfilment center



(c) Shuttle robot

Figure 1.5: Robotics based ASRS

1.2 Stacker Crane Structure

Stacker cranes have two main construction types being single mast and double mast. In the work to be done in this thesis double mast type stacker

crane examined. It is selected due to it being stiffer than the single mast stacker crane in a nutshell. A simple model of a double mast stacker crane shown in the Figure 1.6 with its main components.

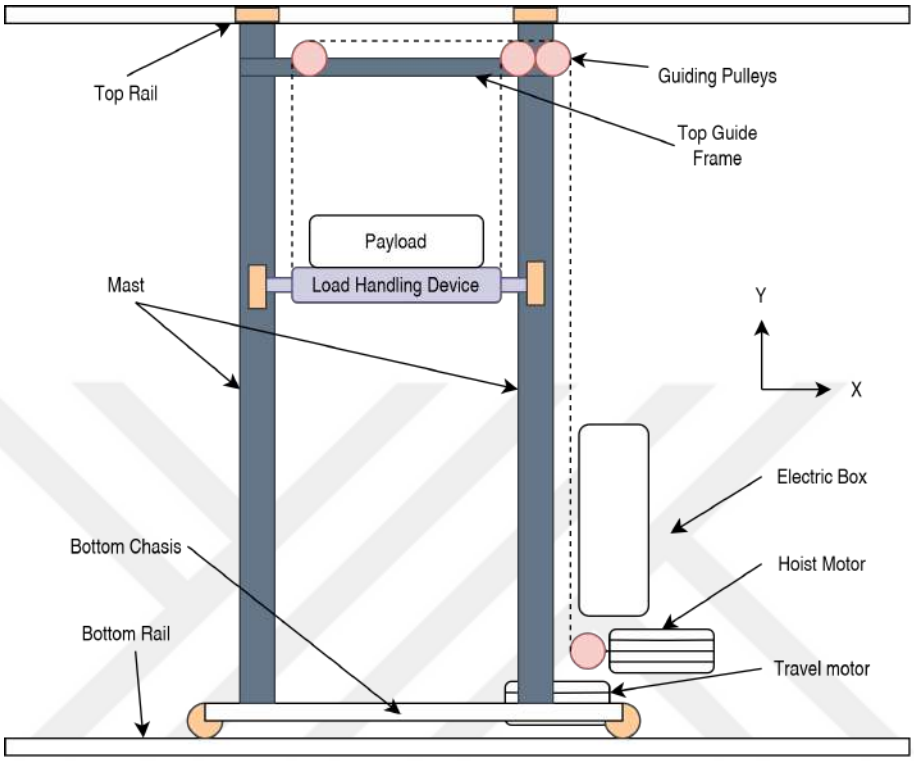

Figure 1.6: Stacker crane components

To briefly explain the structure the main components are the mast, rails and the top and bottom frame. Bottom rail is fixed on the storage floor and the top rail is supported with the rack structure. Rails are used to guide the crane over the aisle. They need to be rigid enough to support the wheel load with the dynamic forces. Rails are commonly selected as H or I profile and train rails. Structure of the stacker crane consists of special welded structures connected with bolts to each other. Stiffness of the stacker crane is based on the mast and bottom/top frame rigidity thus they need to be strong enough not to break under the dynamical loads and also stiff enough not to cause too much vibrations when positioning the crane. The x-axis movement is provided by the torque transmitted to the wheel by the motor. While load handling device (LHD) is positioned by hoist motor via cable and drum equipment. Payload is transferred by the

motor located on the LHD to the rack.

Input and output from the storage system provided by conveyors located at the end of the line, named IO points.

1.3 Literature Survey

Storage algorithms developing with the requirements of the market, herewith the mechanisms required to support this storage algorithms. Stacker cranes are one of the most used machinery in ASRS. Since 1960's they are becoming more efficient, fast and reliable thanks to the academic studies.

There are two main topics that has taken place in stacker crane design and usage of it. First is to determine the storage algorithms and the second one being reducing the vibration of the stacker crane to reduce the positioning time of the machine.

There are many storing algorithms and ASRS design considerations. Companies required to determine the sequence of the storage and retrieval request in order to maximize the performance of the system. First known development of ASRS began with the computational and informational technologies. Calculating the operation time depending on the shape of the rack system has been the first study using Chebyshev distance has done by Hausman et al. (1976) [6]. Bozer and White [2] developed the time travel modes for ASRS machines. Simultaneous movement of both horizontal and the vertical axes of the machine was considered. Randomized storage conditions was used in this study and travel times derived both for single and dual command cycles. Hwang and Lee [7] considered ASRS machine in detail. As the previous work has only considered the average velocity of the machine, it does not take the operating characteristics of the machine itself. Thus, the optimal design and schedule based on the existing models

is far from optimal from the practical point of view. Work done in [7] determined the travel times of single and dual cycle, using randomized assignment policy. Peters et al. [17] examines the problem that where the ASRS machine should dwell (reside / wait) when the system at idle. Paper proposes several analytical models of these expected response times of the AS/RS based on the relative locations of the input and output ports of the AS/RS.

Working field of the ASRS contains high rise structures since the areas in the cities are getting more valuable day by day. Thus stacker cranes need to reach this height to work properly, to optimize the structure weight needs to be minimized. Minimizing weight, introduces a less stiffer structure to be controlled. Therefore, vibrations on the high rise mast of the stacker crane must be controlled in order to achieve efficient operation. Many solutions researched in order to control mast vibrations. Most of them used closed loop control systems and some to use passive damper solutions to reduce the vibration. Since the stacker crane is basically a beam under dynamical loads, the researches based on the classical Timoshenko beam theory [11]. Main theory is that to model the stacker crane as a flexible body as to investigate vibration and deflection. Post et al. stated that if low-vibration reference commands can be generated, then the utility of these systems can be greatly improved [18].To derive a time optimal trajectory generation Staudecker et al. used theory of differential flatness in combination with a finite dimensional approximation of the system to obtain an open loop control law[25]. The only research that found as to model double mast stacker crane is written by Sasaki et al[21]. The equations of motions of the flexible stacker crane system and the boundary conditions are derived. Feedback control of the motion of the flexible stacker crane is derived by considering the time rate of change of the total energy of the system.

1.4 Motivation and Objective

Automated storage and retrieval systems are in the market for a long time as stated in introduction section. Since then, there are many advancements with the state of the art technology, development in materials, control systems, storage assignment algorithms, performance measurements and sequencing of storage and retrieval requests. In this thesis the main focus is on the stacker crane type ASRS, in more detail it's mechanical design and control. Detail of the stacker crane structure and its components are defined in chapter 1.2. No published studies were found for the dynamical forces, selection of mechanical components and loads on the equipment and selection of main components of the stacker crane. Thus, this thesis will be a guide for an engineer to design a stacker crane.

2. Stacker Crane Design

As in most mechanical designs, first the requirements need to be inspected thoroughly. For stacker cranes this requirements should be itemized as, speeds and acceleration of the axes, payload weight and dimensions, corridor length and rack height, rack configuration (Single deep, double deep, multiple deep) and input&output points of the system. Definition of design parameters summarized below;

- **Speed and acceleration:** Speed and acceleration of the axes determined by the cycle/hour. Although the acceleration is limited, there is no theoretical limitation to speed. Fastest stacker cranes in the industry has top acceleration of 3 m/s^2 on x axis and 4 m/s^2 on y (lift) axis. (Axis configurations shown on figure 1.6). System acceleration on x axis is limited by the friction between bottom guide rail and the position of the center of mass of the stacker crane. This topic will be shown in detail in the section 2.4.

- **Payload weight and dimensions:** Payload weights are generally divided around three groups, to 100 kg is miniload, to 500kg is midiload and to 1500 kg heavy load. 100-kilogram products usually consist of boxes, while 1500-kilogram products are in pallets. Storage units may change based on customer requirements. There are also some extreme examples the payload of which is a car chassis.



(a) Box Stacker Crane (Jungheinrich)



(b) Pallet Stacker Crane (Mecalux)

Figure 2.1: Stacker crane payload configurations

- **Corridor length and rack height:** Today, shelf heights reach 50 meters and the length of the corridors are past 100 meters. The reach of the stacker crane to the top and the bottom rack is the most important one since that determines the dead space over the corridor length. Tolerances of these payloads are stored in the rack and the general tolerances are given in the standard FEM 9.832 [4].

- **Rack configuration:** General configurations are single deep and double deep rack system. Depth means that how many goods are stacked in a single cell of a rack. Since single deep rack system gives the advantage of getting the highest throughput, double deep stacked goods yield a high balance between storage capacity and processing speed. With double deep stacker crane, twice the number of goods can be stored in an aisle. Although, it has a disadvantage as the stacker crane cannot reach the good in the second depth if there is a good in front

of it.

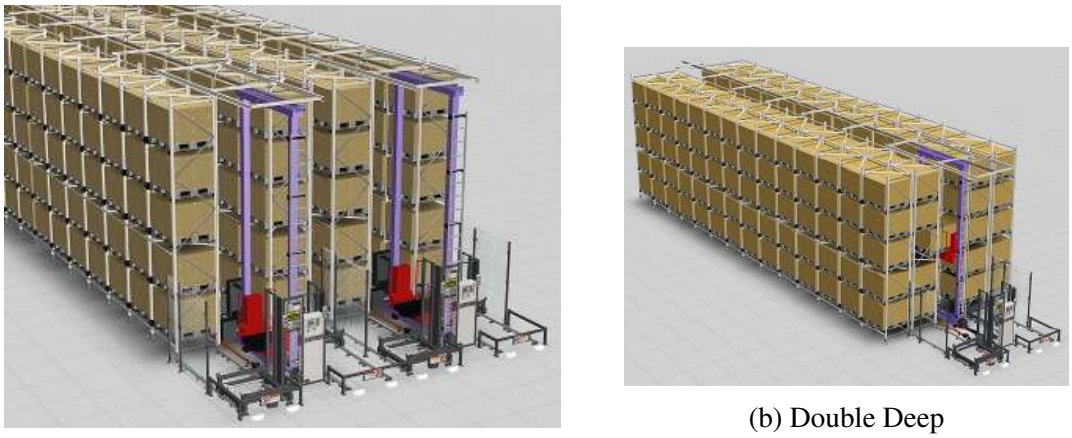

(a) Single Deep

(b) Double Deep

Figure 2.2: Stacker crane racking configurations

2.1 Mast Construction Determination

Construction of the mast of the stacker crane plays a critical role in either determining the stresses and vibration of the stacker crane. Main loads acting on the mast are caused by the acceleration on the x axis. When accelerating the weight of itself and the weight of the load handling unit acts as a force on the mast. Mast construction is simply a beam under dynamical loads. It is also looks like an inverted pendulum with rigid joint.

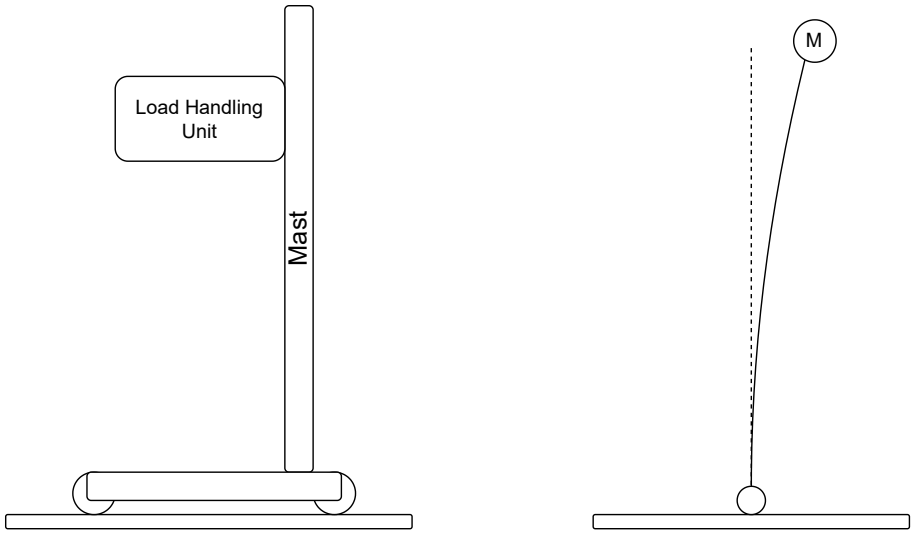

Figure 2.3: Stacker Crane and Inverted Pendulum

Since the stacker crane works with high rack structures, one must de-

termine its rigidity in order to create a control algorithm for the vibration caused by high velocity operation. There is also a trade-off between rigidity and unit mass of the mast structure. Thus; one must design a mast that has high rigidity with low unit mass. There are some researches like, designing a mast with highly damped fibre-reinforced lightweight structure [5] and periodic topology optimization of a stacker crane [8]. Currently, aluminium and steel structures are used in mast design in stacker crane with active vibration control devices.

Other critical design consideration is that to determine the mast quantity in the stacker crane. There are two main constructions being single mast and double mast stacker crane. Rigidity along the x axis (Along aisle) is the most important parameter of the structure. Although single mast stacker crane is easier to construct, it is not preferred in heavy duty applications. The reason being that the double mast stacker crane is more rigid with same weight.

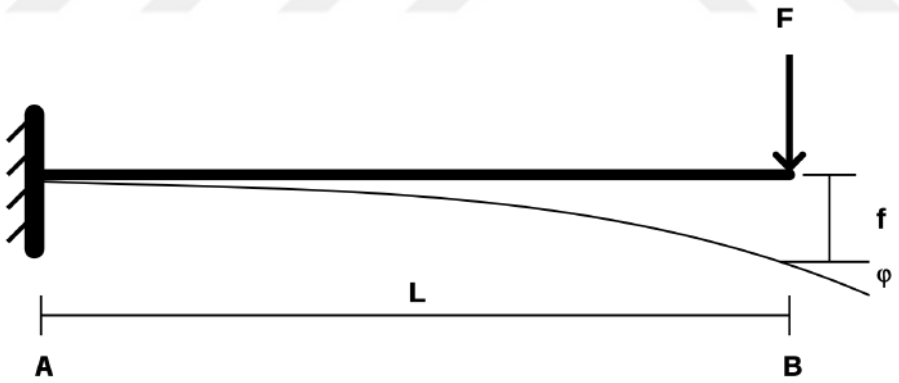

Figure 2.4: Deflection of a simply supported beam

Stiffness of a beam defines how much the beam resist to deflection. Force F, is the inertial load of the LHD and f is the deflection created by that force. f_{max} is determined by the formula below; E is elastic modulus of the material, I is second moment of area about the neutral axis and L is the length of the beam.

$$f_{max} = \frac{F \cdot L^3}{3 \cdot E \cdot I} \tag{2.1}$$

Since stiffness means a beam's ability to resist deflection, formula can be rearranged with k being stiffness;

$$k = \frac{F}{f_{max}} = \frac{3 \cdot E \cdot I}{L^3} \tag{2.2}$$

Simply supported beam represents the single mast stacker crane. Although generally Euler-Bernoulli beam theory is used to represent the model of the crane, lowest natural frequency of the structure can be found by simplifying the continuous beam model to a single degree of freedom system.

Double mast stacker can be modeled as a single story structure and its stiffness can be obtained by using analysis of lateral stiffness of a one story frame, thus finding a equivalent spring constant for the stacker crane structure. Main difference between the single mast and double mast stacker crane structure is that, with double mast configuration, at the tip of the mast rotation of the beam is being reduced by the lateral beam in between two masts. For a uniform beam with either ends is fixed against rotation, stiffness defined by $k = \frac{12 \cdot E \cdot I}{L^3}$ [12], against the beam with one end fixed and the other is free has the stiffness of $k = \frac{3 \cdot E \cdot I}{L^3}$[12].

The profile chosen for the mast is given below. Selection of this profile depends on ease of use with its slotted design, scalability for higher stacker crane designs with similar profiles with bigger sizes and higher inertial properties and for its material being aluminium, thus having lower weight per meter ratio over metal materials.

Properties of 80x240 sigma profile;

Area	7422	mm^2
I_x	540.8	cm^4
I_y	4268.2	cm^4
W_x	135.2	cm^3
W_y	355.7	cm^3
Weight	20015	g/m

Table 2.1: Parameters of mast profile



(a) Isometric View

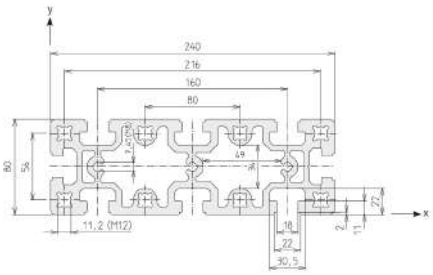

(b) Cross Section and Dimensions of the Profile

Figure 2.5: Rose+Kriger D-80x240 Aluminium Sigma Profile

2.2 Stacker Crane Parameters

Parameters of the stacker crane in this project was determined by the research on existing cranes in the market. Determined parameters given below;

X Axis Speed	5	m/s
X axis acceleration	3	$m/^2$
Y axis speed	4	m/s
Y axis acceleration	4	m/s^2
Z axis Speed	2	m/s
Z axis acceleration	2	m/s^2
Payload	100	kg

Table 2.2: Parameters of stacker crane

2.2.1 Lateral Stiffness of The Double Mast Stacker Crane

The structure of the double mast stacker can be solved with structural dynamics equations. The important parameter to extract from these solutions is that the lateral stiffness of the system. With finding lateral stiffness of the system, we can create a virtual spring between the bottom carriage and the top guide. In this analysis LHD assumed to be at top position in fact it is assumed to be single mass with the top guide. Also the weight of the columns reduced to the top guide, without changing the total energy of

the system. This will be explained in detail, in later of this section.

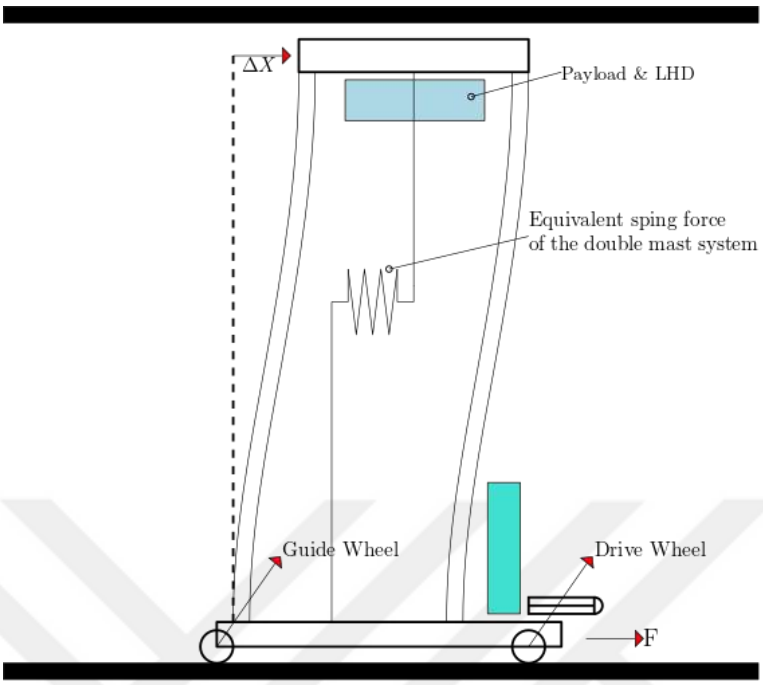

Figure 2.6: Deformation of Double Mast Stacker Crane

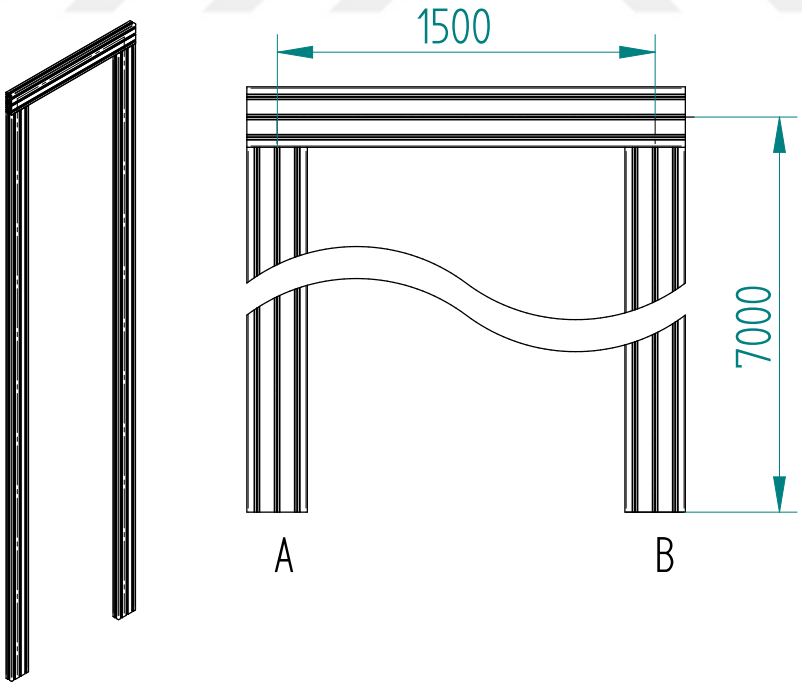

Figure 2.7: Left: Isometric view Right:Dimensions of Stacker Crane

Lateral stiffness of the stacker crane could be found with the equations

with stiffness of beam elements. The stiffness of the beam with both ends fixed is given[26];

$$k = 12\frac{E \cdot I}{L^3} \tag{2.3}$$

For each beam of the stacker crane calculated as;

$$k_{beam} = 12 \cdot \frac{70\,GPa \cdot 4268\,cm^4}{7000\,mm} = 104.52\,kN/m \tag{2.4}$$

Total stiffness of the springs in parallel;

$$k_{equivalent} = k_1 + k_2 \tag{2.5}$$

Thus, total stiffness of the double mast stacker crane is approximately;

$$k_{equivalent} = 2 \cdot k_{beam} = 2 \cdot 104.52 = 209\,kN/m \tag{2.6}$$

Deriving a mathematical model is the base for controlling a system. It creates a mathematical function that represents how the system behave with the input signal. Therefore, controlling the stacker crane, one must develop a mathematical model for the crane. In order to derive a mathematical model, the spring coefficient, damper coefficient and masses in the system must be known. Equivalent spring coefficient of the double mast stacker crane generated in 2.6.

To find the natural frequencies of the system we can use the Rayleigh's quotient. Theorem says the natural frequencies of a system can be found by taking ratios of the system energies [26]. The stacker crane assumed to be a beam with a lumped mass in the end. Stacker crane's mast are the beam and the LHD is the lumped mass in this assumption.

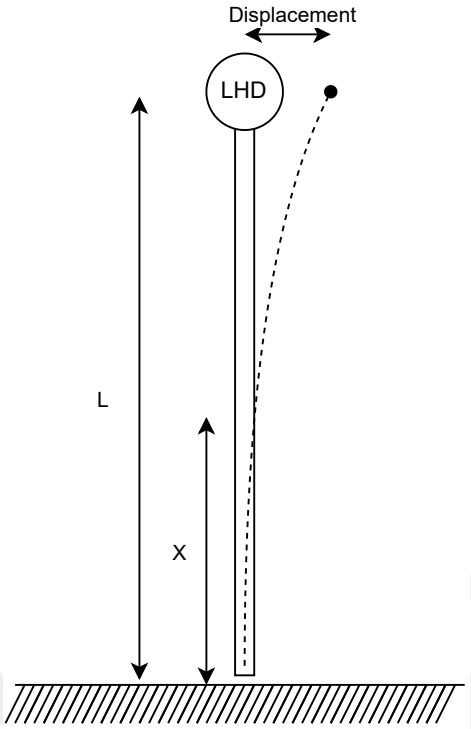

Figure 2.8: Assumed model of stacker crane

Kinetic energy of a generic system is given by;

$$KE = \frac{1}{2} m \cdot \delta^2(L) \tag{2.7}$$

δ is the displacement and the KE is the kinetic energy in the equation above.

In stacker crane the weight of the mast is not insignificant to not take into account when finding the natural frequency. Assuming the velocity distribution in the mast is linear through the height then we'd have;

$$\dot{\delta}(x) = \frac{x}{L} \dot{\delta}(L) \tag{2.8}$$

In reality the actual distribution cannot be precisely linear. The larger the tip mass of this kind of system, the first mode will be closer to a linear distribution, and the closeness will degrade as the end mass is reduced with respect to the mast's mass. Taking mast's mass into account, the kinetic

energy becomes;

$$KE' = \frac{1}{2} M_{LHD} \dot{\delta}^2(L) + \frac{1}{2} \int_0^L \rho \dot{\delta}(x) dx \tag{2.9}$$

Using 2.8;

$$KE' = \frac{1}{2} M_{LHD} \dot{\delta}^2(L) + \frac{1}{2} \int_0^L \rho (\frac{x}{L})^2 \dot{\delta}^2(L) dx \tag{2.10}$$

Arranging;

$$KE' = \frac{1}{2} \dot{\delta}^2(L)(M_{LHD} + \int_0^L \rho (\frac{x}{L})^2 dx) \tag{2.11}$$

Evaluating integral;

$$KE' = \frac{1}{2}(M_{LHD} + \frac{\rho \cdot L}{3}) \dot{\delta}^2(L) \tag{2.12}$$

Comparing 2.7 and 2.12 it is seen that the mass of the mast is added to the equation, therefore the system now have a equivalent mass at the tip of the stacker crane. M_{LHD} is taken $300\,kg$. Which calculates as $M_{LHD} + \frac{\rho L}{3}$, 346kg.

2.3 Finite Element Analysis of the Mast

To confirm what is found in analytical calculations finite element method is a powerful tool to use in analysing structures. Double mast stacker crane structure shown in 2.7 analyzed in NX Advanced [23]. 1-D elements are used to represent the profile given in 2.5. Cross section of the profile given to the program as an input and its inertial properties calculated by program. Boundary conditions are that the stacker crane fixed from A and B points. Total of 152 elements and 150 nodes are used in the analysis.

FEA (Finite element analysis) is used to find the reaction forces and moments at beam connection points in order to select or design the required

mechanical connection elements to those beams. In working conditions the structure undergo acceleration forces created by motors in the system and the gravity. Weight of the LHD estimated to be $300kg$ with the payload, thus with the $3m/s^2$ acceleration on the x axis, it creates $900N$ force on the structure. Force assumed to be acting on the top bar of the stacker crane in the analysis in order to simulate worst case scenario. Boundary conditions are same as the previous analysis.

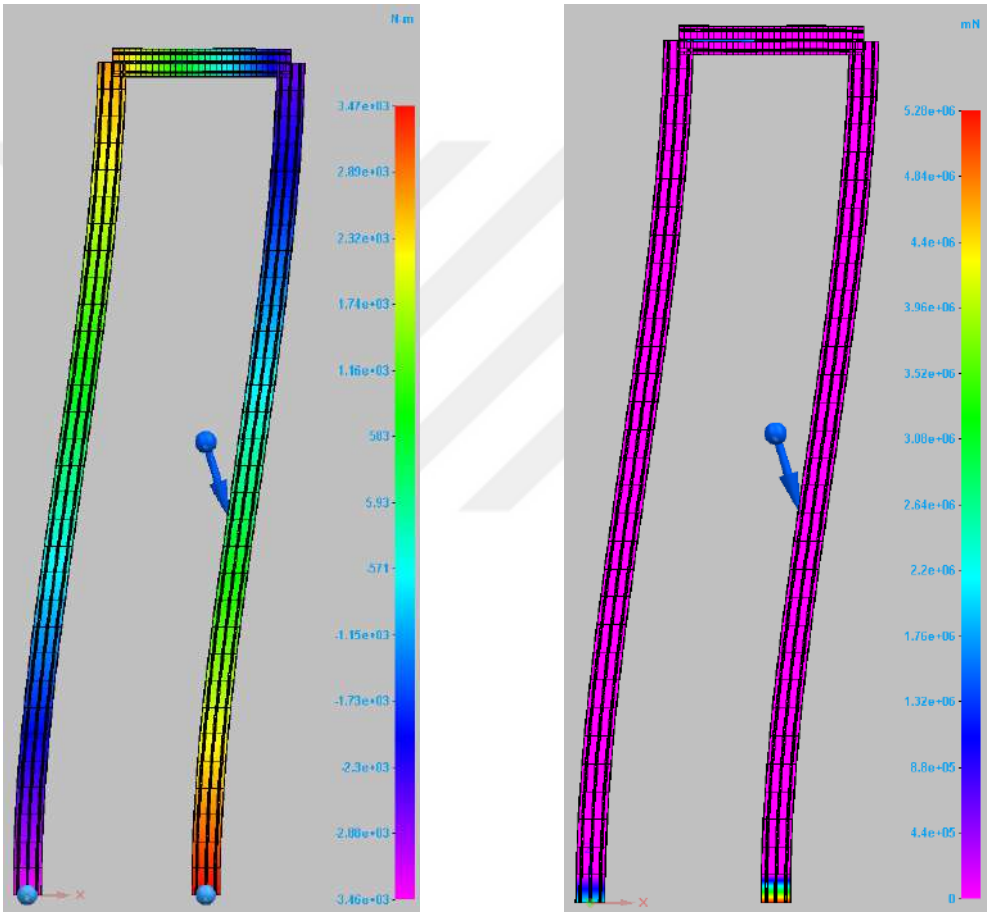

(a) Reaction moments (b) Constraint forces

Figure 2.9: Resultant moment and constraint forces on beams

Results from FEA are shown below;

Reaction moments at bottom connection	$\pm$3470	Nm
Reaction moments at top bar connection	$\pm$2640	Nm
Constraint force of beam B	5280	N
Constraint force of beam A	2130	N

Table 2.3: FEA results

It is also seen that the shape of the top bar is not changed significantly, thus not disturb the assumed parallel springs method. If the top bar has changed its shape, it creates rotation around the joint, hence disturbing our assumption that has been made as the each section of mast stands between two fixed points.

To connect the profiles to each other and the bottom frame it is critical to ensure that the connection elements needs to maintain structural integrity according to the found reaction moments and constraint forces in 2.9. The supplier of the profiles [9] also supplies the right angle connectors for the profiles. The connector can carry 3000 Nm moment force with 3000 N shear force. Thus, with 2 connector used in bottom of the profile and 1 connector used in top profile, stability of the structure is ensured.

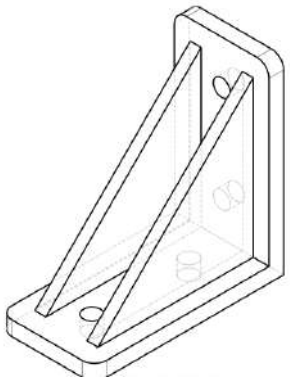

Figure 2.10: Right angle connector [9]

Natural frequency of the stacker crane can be calculated via modal analysis module. For this purpose Solid Edge is used to model the stacker crane with 1-D beam elements. 1200kg weight is added to the bottom beam to represent the weight of all the elements that are carried by the bottom frame and 300kg is added to the top beam as to represent the weight of the LHD and the payload. Results are shown in the figure below.

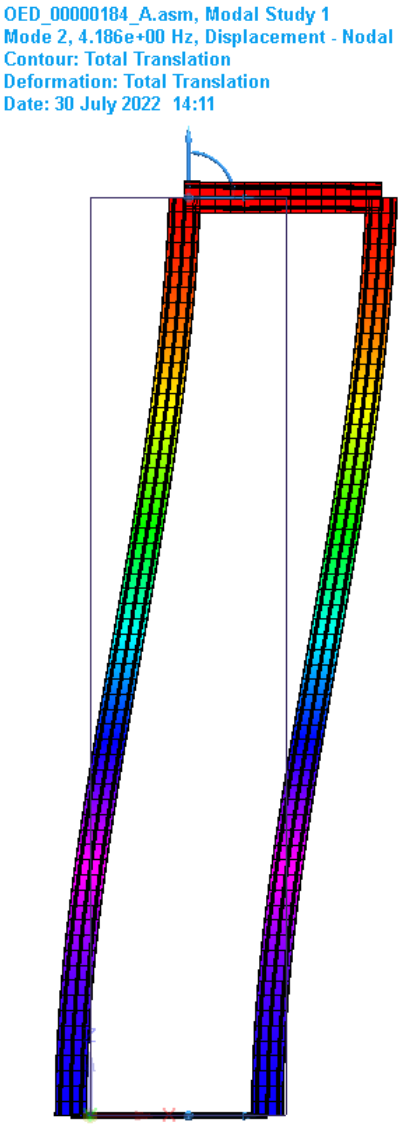

Figure 2.11: 1st resonance mode of stacker crane structure

First mode resonance frequency is found 26.26 Rad/sec on the analysis done. The difference between analytical calculations and the FEA model is caused from the differences in properties of the beam element calculated by the program using the solid model taken from the manufacturer and joint stiffness of the beams.

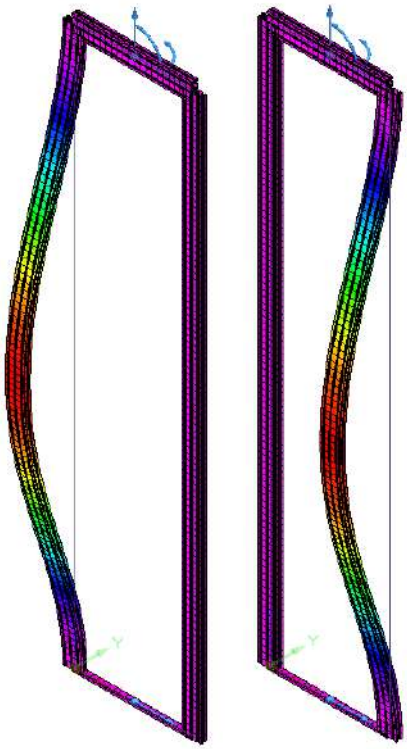

Figure 2.12: 2nd and 3rd resonance mode of stacker crane structure

Second and third resonance of the stacker crane is given in the figure 2.12. Those resonance modes occur at $60 rad/sec$ and expected to be damped depending on the properties of the material.

2.4 Dynamic Analysis of the Structure

Determined accelerations of the stacker crane given in 2.2. Although there are specified parameters, the x-axis acceleration is limited by the structure of the system, the friction of the wheels and the position of the center of gravity. Structure of the system described in 1.6. A standard stacker crane is driven by the load carrying wheels attached to the motor or motors. One-wheel drive system is more preferred due to economic reasons. The double wheel drive configuration is used in order to achieve higher accelerations. There are also some designs that are not driven by

the load carrying wheel but other drive mechanisms like, belt&pulley and rack&pinion. An example of Mias' stacker crane is given below [15]. It is driven with omega drive configuration that uses belt&pulley mechanism. The downside of this system is that there has to be a belt running along the corridor.

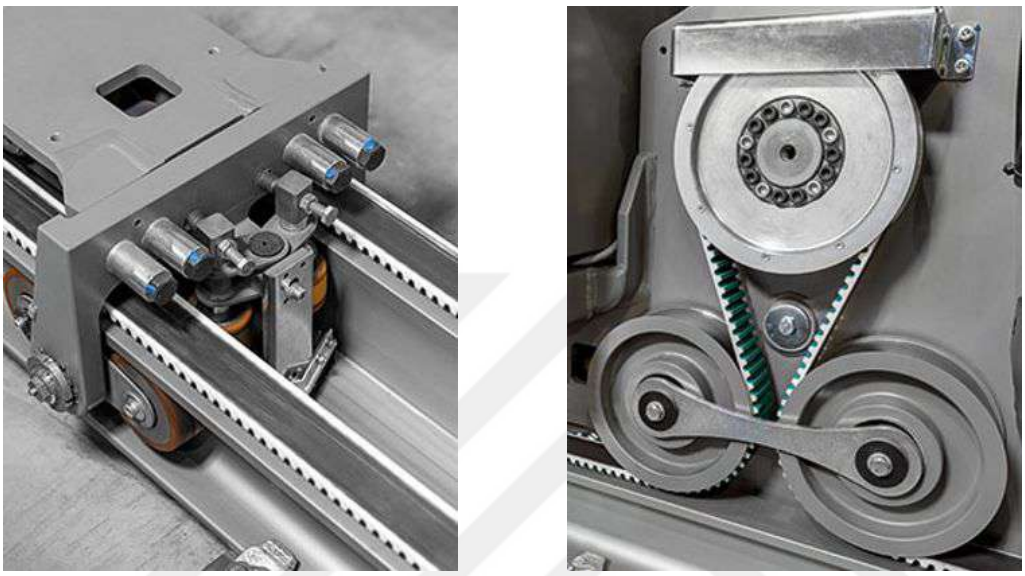

(a) Track rail (b) Omega drive

Figure 2.13: Drive configuration of mias miniload stacker crane [15]

Determining the limitation acceleration of the stacker crane's x axis, one must consider the load on the drive wheel. A wheel's maximum drive force / lateral force is determined by the load acting on it and the friction between the wheel and the surface it's on. Lateral drive force of the wheel cannot be bigger than static friction force. Drive wheel used in this study has 200mm diameter, vulkollan material and has a 0.35 friction coefficient between the wheel and steel. Friction coefficient of the wheel is given by the supplier.

The load acting on the wheel is actively changing with the acceleration of the stacker crane. Calculating the load on the wheel depends on the center of mass of the crane and the distances given in 2.14.

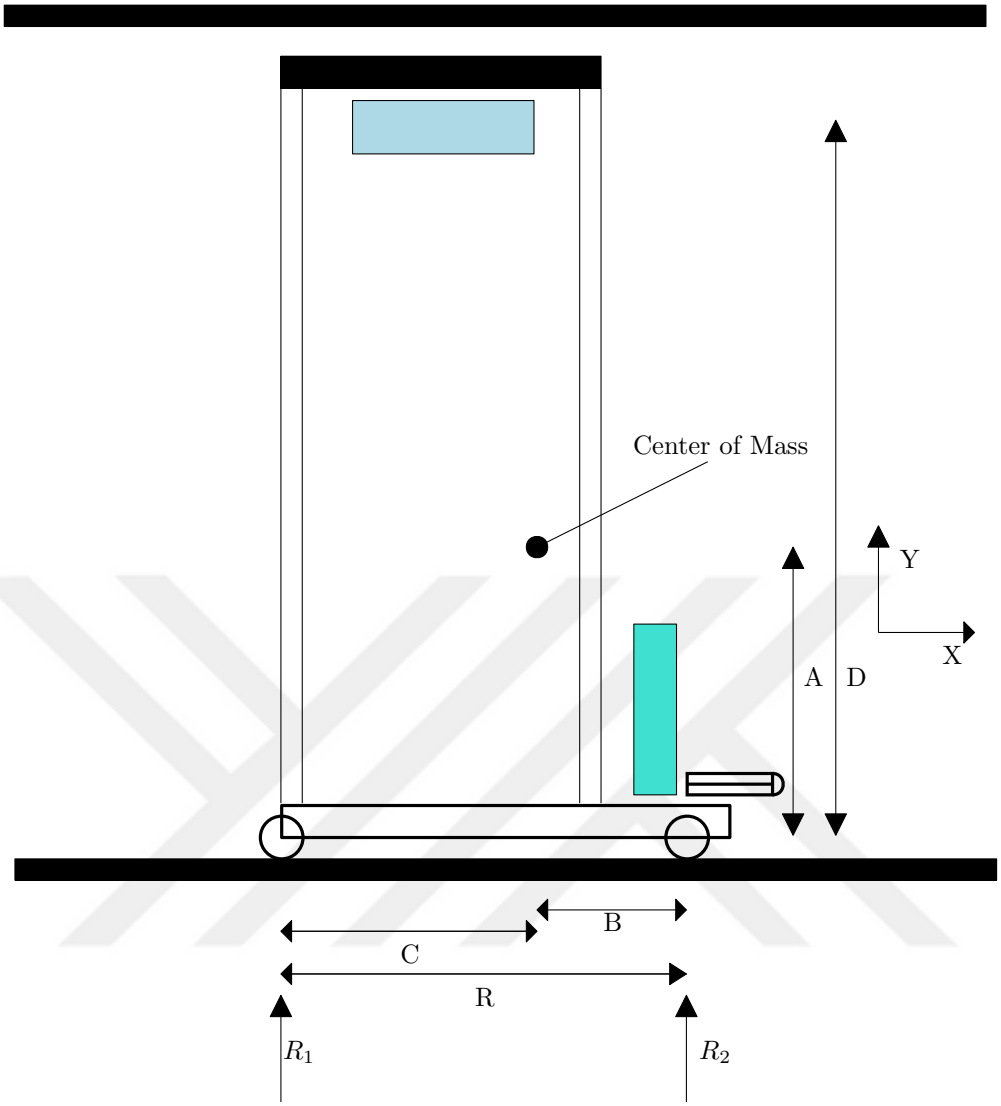

Figure 2.14: Dimensions of stacker crane according to center of mass

R_1 and R_2 are the reaction forces of the load carrying wheels. Wheel loads of the stacker crane could be found with taking moment around wheel R_1. In equilibrium conditions moment around R_1 should be zero, thus the reaction force of the wheels could be calculated. A, B, C represents the distances between center of gravity and wheels, D represents the distance between wheel height and LHD with payload and R represents the distances between two wheels. M is the total weight of the stacker crane, including motors and payload. a_x is the acceleration on x axis. Remembering that, if a mass is accelerating there is a force acting on it by Newton's second law $F = M \cdot a$.

Accelerating in +x axis; (Counter Clockwise moments taken positive)

$$M_{R_1} = A \cdot M \cdot a^{+x} + R_2 \cdot R - M \cdot C \cdot g \tag{2.13}$$

Accelerating in -x axis;

$$M_{R_1} = -A \cdot M \cdot a^{-x} + R_2 \cdot R - M \cdot C \cdot g \tag{2.14}$$

In an equilibrium the moment around wheels is zero. Accelerating in +x axis;

$$0 = A \cdot M \cdot a^{+x} + R_2^{+x} \cdot R - M \cdot C \cdot g \tag{2.15}$$

Accelerating in -x axis;

$$0 = -A \cdot M \cdot a^{-x} + R_2^{-x} \cdot R - M \cdot C \cdot g \tag{2.16}$$

In either of this equations, the traction forces of accelerations a^{+x} and a^{-x} must be under the traction force that the drive wheel can apply. F_t^{+x} is traction force for $+x$ axis and F_t^{-x} is traction force for $-x$ axis. The traction force of the stacker crane calculated as;

$$\begin{aligned} F_t^{+x} &= R_2^{+x} \cdot \mu_k \\ F_t^{-x} &= R_2^{-x} \cdot \mu_k \end{aligned} \tag{2.17}$$

Remembering the maximum traction cannot be higher than the load on the wheel, multiplied with friction.

$$\begin{aligned} R_2^{+x} \cdot \mu_k &\leq M \cdot a^{+x} \\ R_2^{-x} \cdot \mu_k &\leq M \cdot a^{-x} \end{aligned} \tag{2.18}$$

Leaving reaction force alone gives;

$$\begin{aligned} R_2^{+x} &\leq \frac{M \cdot a^{+x}}{\mu_k} \\ R_2^{-x} &\leq \frac{M \cdot a^{-x}}{\mu_k} \end{aligned} \tag{2.19}$$

Inserting 2.19 into 2.15 and 2.16;

$$\begin{aligned} 0 &= A \cdot M \cdot a^{+x} + \frac{M \cdot a^{+x}}{\mu_k} \cdot R - M \cdot C \cdot g \\ 0 &= -A \cdot M \cdot a^{-x} + \frac{M \cdot a^{-x}}{\mu_k} \cdot R - M \cdot C \cdot g \end{aligned} \tag{2.20}$$

The mass in both equations cancel out, leaving;

$$\begin{aligned} 0 &= A \cdot a^{+x} + \frac{a^{+x}}{\mu_k} \cdot R - C \cdot g \\ 0 &= -A \cdot a^{-x} + \frac{a^{-x}}{\mu_k} \cdot R - C \cdot g \end{aligned} \tag{2.21}$$

Rearranging the equations, leaving accelerations alone;

$$\begin{aligned} a^{+x} &= \frac{C \cdot g}{A + \frac{R}{\mu_k}} \\ a^{-x} &= \frac{C \cdot g}{-A + \frac{R}{\mu_k}} \end{aligned} \tag{2.22}$$

As can be seen from the equation 2.22, the parameters affecting the maximum acceleration are the distances of the wheels from center of mass and the coefficient of the friction.

In the design work carried out considering the weight distribution of the system, the electrical panel, motors and similar equipment were placed close to the R_2 wheel in order to maximize the acceleration. With parameters given below, maximum a^{+x} and a^{-x} could be calculated.

A	2500	*mm*
B	1000	*mm*
C	2000	*mm*
R	3000	*mm*

Table 2.4: Dimensions of center of mass and load carrying wheels

Taking $g = 9.81$ and $\mu_k = 0.35$, maximum accelerations are;

$$
\begin{aligned}
a^{+x} &= \frac{2000 \cdot 9.81}{2500 + \frac{3000}{0.35}} = 1.77 \frac{m}{s^2} \\
a^{-x} &= \frac{2000 \cdot 9.81}{-2500 + \frac{3000}{0.35}} = 3.23 \frac{m}{s^2}
\end{aligned} \tag{2.23}
$$

Distance A in figure 2.14, is the distance between the wheel and the center of mass in y axis. The center of the mass position on the x-y plane changes with the position of the LHD. Since LHD can move between the top and bottom rack in y axis, the distance A changes between $2500\,mm$ and $2400\,mm$. Therefore, a^{+x} and a^{-x} accelerations have an interval for maximum accelerations. Taking 2.22 one could find these interval as;

$$
\begin{aligned}
1.77 \frac{m}{s^2} < a^{+x} < 1.79 \frac{m}{s^2} \\
3.18 \frac{m}{s^2} < a^{-x} < 3.23 \frac{m}{s^2}
\end{aligned} \tag{2.24}
$$

2.4.1 Wheel Loads

To size the wheels in the system, the loads on the wheel must be found. With the accelerations found in 2.23, maximum load on wheels could be found with moment equilibrium equations 2.14 and 2.13. Mass of the stacker crane in total with payload is $1800kg$.

Accelerating in +x axis;

$$
\begin{aligned}
0 &= A \cdot M \cdot a^{+x} + R_2^{+x} \cdot R - M \cdot C \cdot g \\
0 &= 2500 \cdot 1800 \cdot 1.79 + R_2^{+x} \cdot 3000 - 1800 \cdot 2000 \cdot 9.81 \\
R_2^{+x} &= 9087\,N
\end{aligned} \tag{2.25}
$$

$$
R_1^{+x} = M \cdot 9.81 - R_2^{+x} \tag{2.26}
$$

$$
R_1^{+x} = 8571N \tag{2.27}
$$

Accelerating in -x axis;

$$
\begin{aligned}
0 &= -A \cdot M \cdot a^{-x} + R_2^{-x} \cdot R - C \cdot M \cdot g \\
0 &= -2500 \cdot 1800 \cdot 3.23 + R_2^{+x} \cdot 3000 - 1800 \cdot 2000 \cdot 9.81 \\
R_2^{-x} &= 16617N
\end{aligned} \tag{2.28}
$$

$$R_1^{-x} = M \cdot 9.81 - R_2^{-x} \tag{2.29}$$

$$R_1^{-x} = 1041N \tag{2.30}$$

R_1 wheel has maximum load of $8571N$ and R_2 wheel has maximum load of $16617N$. With taking safety factor 1.5 and taking the speed of $5m/s$ for both wheels, following wheel are selected. Drive wheel with a keyway is selected for R_2 wheel and R_1 wheel is a guide roller that has no keyway and with integrated bearings.



(a) R_1 Guide roller (b) R_2 Drive Wheel

Figure 2.15: Wheels of stacker crane [28]

2.5 Motor Selection and Cycle Calculation

To select a suitable motor for a system several parameters should be defined carefully. These parameters being motor maximum rotational speed, peak torque and RMS torque required in a cycle. There are also some miscellaneous hardware that to be selected like the encoder type, brake

requirement for the system, cable technology, cooling type and etc.

While selecting the motor, the duty cycle should be determined first. Duty types explained below;

- Continuous duty (S1): Motor is loaded with constant load, the duration of loading lets the motor reach the thermal equilibrium. As an example of a S1 duty, that the motor is turned on with a fan coupled to it and then let it run non-stop. Advantages of continuous duty cycle that it is efficient while motor runs its dedicated rpm, dependable, and simple. Example usage areas are escalators, packing machines and conveyor belts.

- Short time duty (S2): Motor runs under a load for a brief time period. The period ends before the motor reaches the thermal equilibrium. Then the motor rests for a while to let it cool for the duration. With S2 time duty motors can be used higher than its nominal torque for a period of time. The length of this period is determined by its manufacturer. It can be also determined that how many cycles that the motor can run in a period of time; like 4 runs in a minute.

- Periodic duty (S3): This duty cycle includes changing loads with changing speeds. The various processes of the cycle are repeated over time and the motor is not allowed to reach thermal equilibrium. It is the most used duty cycle in robotics; positioning systems, mobile robots, linear and rotary actuating systems runs with this duty cycle. Root mean squared (RMS) torque should be calculated for stacker crane's operation. RMS torque is equivalent to the nominal torque of the motor. To calculate the RMS torque for the system, one must determine a cycle and calculate the required motor torque output for each segment of the cycle. The calculation of the RMS torque can differ for each manufacturer but the general formula given in 2.31. M

is torque and t is the time in each section and t_e is the total time of the cycle.

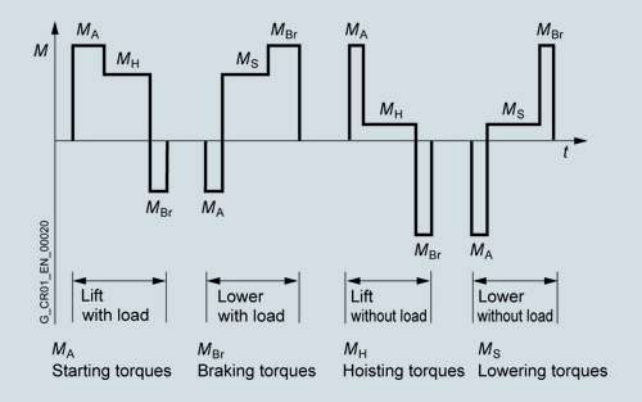

Figure 2.16: Typical torque diagram for hoist across one conveying cycle [22]

$$M_{RMS} = \sqrt{\frac{\sum M^2 \cdot t}{t_e}} \tag{2.31}$$

2.5.1 RMS Torque Calculation

There are lots of cycles could be created for a stacker crane for each payload to be transferred in and out. In addition to that cycle policies can change due to requirements for the ASRS. As different policies and different analysis for a cycle done in [27] single command cycle taken for simplicity.

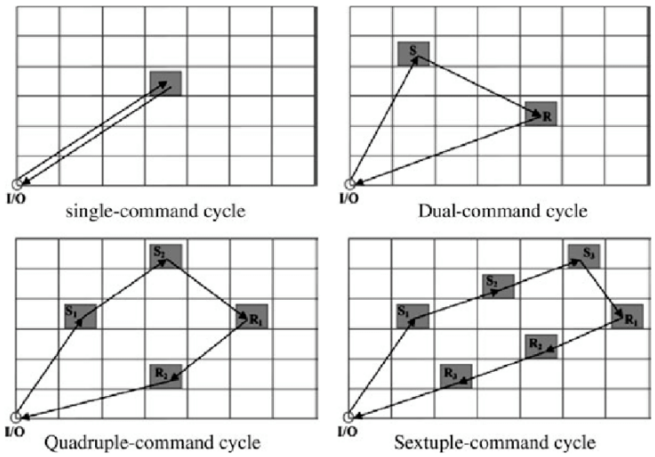

Figure 2.17: Different command cycles of the stacker crane [27]

Single command cycle has the following segments.

For x axis;

1. +x acceleration
2. constant speed
3. +x deceleration
4. Pick & Place waiting time
5. -x acceleration
6. constant speed
7. -x deceleration

For y axis;

1. +Y acceleration
2. constant speed
3. +y deceleration
4. Pick & Place waiting time
5. -y acceleration
6. constant speed
7. -y deceleration

2.5.1.1 RMS Torque calculation for X axis

X axis is the axis along the aisle as shown in figure 1.6. In the configuration shown in figure 1.6 a single wheel accelerates the stacker crane. Accelerating force applied to the system by the wheel is a lateral force along x

axis. Lateral force converted to torque force by the wheel. By using gearbox, torque is reduced and the rotational speed is increased. Drive-train schematics of x axis is given below.

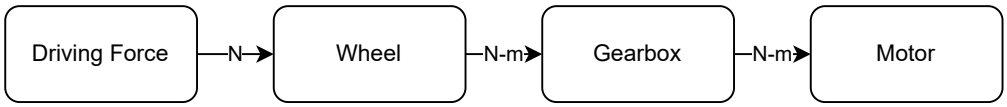

Figure 2.18: X axis drive-train

Driving force of each section is calculated with the following formula; A is used for acceleration and D is used for deceleration.

$$F_{drive} = M \cdot a \tag{2.32}$$

Maximum accelerations were found in 2.23 as $1.77 m/s^2$ in a^{+x} and $3.23 m/s^2$ in a^{-x} and the total weight of the system is $1800 kg$. Thus, with these information the drive force required can be calculated.

Converting drive force to wheel torque is simple with the equation given below. Drive force multiplied with wheel radius gives the required torque on the wheel input. The wheel is selected, with the results from 2.27 and 2.30, it has 250mm diameter and can carry 10 ton at 5 m/s.

$$\tau_{wheel} = F_{drive} \cdot r_{wheel} \tag{2.33}$$

Torque input to the wheel is connected to the gearbox output. The gearbox output torque is proportional to the input shaft torque according to the gear ratio. With the efficiency of the gearbox it is calculated as following;

$$\tau_{wheel} = \tau_{gearboxinput} \cdot i \cdot \eta_{gearbox} \tag{2.34}$$

Using the equations 2.32, 2.33 and 2.34 and adding motor efficiency gives the following equation for calculating motor torque. η_{motor} and $\eta_{gearbox}$ are taken 0.95.

$$\tau_{motor} = \frac{\tau_{wheel}}{i} / (\eta_{motor} \cdot \eta_{gearbox}) \tag{2.35}$$

$$\tau_{motor} = (\frac{F_{drive} \cdot r_{wheel}}{i}) / (\eta_{motor} \cdot \eta_{gearbox}) \tag{2.36}$$

$$\tau_{motor} = (\frac{Mass \cdot A \cdot r_{wheel}}{i}) / (\eta_{motor} \cdot \eta_{gearbox}) \tag{2.37}$$

Since the system uses a gearbox, the same ratio as the torque scaled down, speed the scaled up. The rotational speed of the wheel must be found first.

$$\omega_{wheel} = \frac{Linearspeed}{Wheelcircumference} \cdot 60 \tag{2.38}$$

$$\omega_{wheel} = \frac{V_x}{\pi \cdot D} \cdot 60 \tag{2.39}$$

Motor RPM is the wheel RPM multiplied by gearbox ratio;

$$\omega_{motor} = \omega_{wheel} \cdot i \tag{2.40}$$

$$\omega_{motor} = \frac{V_x}{\pi \cdot D} \cdot 60 \cdot i \tag{2.41}$$

With equations 2.41 and 2.37 we can calculate the motor requirements in acceleration segments. In pick & place waiting times motor speed and torque is zero. Only constant speed segments are remained to calculate. The parameter that creates the biggest load on the motors when going at a constant speed is the rolling resistance. Rolling resistance is a measure of the retarding effect of a floor surface at the tread/floor interface of the wheels. It is normally expressed in pounds and is a measure of the energy dissipated per unit of distance rolled. Rolling resistance calculated as

follows;

$$F_{Rolling\,resistance} = f_{rolling} \cdot \frac{W}{R} \tag{2.42}$$

Where $f_{rolling}$ is coefficient of rolling friction, $F_{rolling\,resistance}$ is the force required to overcome the rolling friction, W is the load on the wheel and R is the radius of the wheel. $f_{rolling}$ is given 0.040 for polyurethane wheel and steel in inch unit.

Thread Material	Floor Material	Coefficient of Rolling Friction (inches @ 3mph)
Forged steel	Steel	0.019
Cast Iron	Steel	0.021
Hard Rubber	Steel	0.303
Polyurethane	Steel	0.030-0.057
Cast Nylon	Steel	0.027
Phenolic	Steel	0.026

Table 2.5: Rolling friction of different materials [3]

$$F_{Rolling\,resistance} = 0.04 \cdot \frac{1800 \cdot 9.81}{4.92''} = 143.6N \tag{2.43}$$

Finally, the gearbox ratio should be selected in order to completely calculate each segment of a cycle. Selected gearbox should be ensure that the motor can reach the wheel speed. In this kind of applications where bigger sized motors are used, Siemens suggests that the customer should be using asynchronous servo motors, which generally have 3000 RPM general speed ratings. Since, ω_{wheel} is found to be 381 RPM, with 2.39, required gearbox ratio is 7.87. It is taken 8 to make it easier to find a gearbox.

To calculate the segment durations, length of the motion in x axis is taken 20 meters. Stacker crane assumed to be given a trapezoidal motion profile. In trapezoidal motion object is accelerated to its maximum speed and it travels in the maximum speed for a duration of time, then decelerates to a full stop.

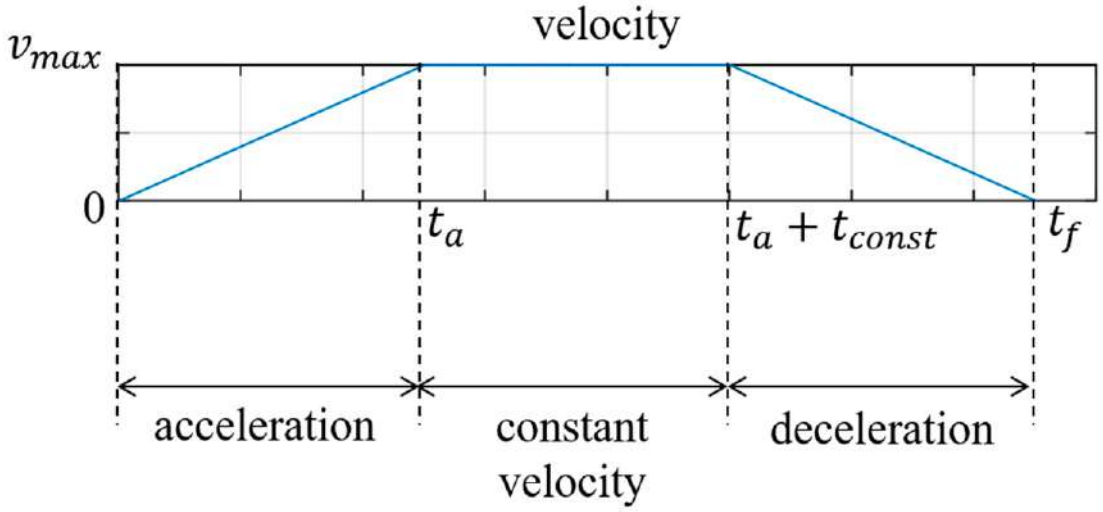

Figure 2.19: Trapezoidal motion profile [29]

Distance covered in acceleration and deceleration calculated as;

$$X = \frac{1}{2} \cdot a \cdot t^2 \tag{2.44}$$

Where X is the distance covered, a is the acceleration and t is the time. For our assumed motion for 10 meters, time for segment 1 & 7 calculated as;

$$X = \frac{1}{2} \cdot 1.77 \cdot t^2 \tag{2.45}$$

Since t is the time to reach the desired speed;

$$T = \Delta V / a \tag{2.46}$$

for segment 1 & 7;

$$T_{1\&7} = 5/1.77 = 2.82 second \tag{2.47}$$

And the distance covered;

$$X_{1\&7} = \frac{1}{2} \cdot 1.77 \cdot 2.82^2 = 7.03m \tag{2.48}$$

Time required to complete the segments 3 % 5 is;

$$T_{3\&5} = 5/3.23 = 1.54s \tag{2.49}$$

And the distance covered;

$$X_{3\&5} = \frac{1}{2} \cdot 3.23 \cdot 1.54^2 = 3.83m \tag{2.50}$$

Thus to calculate constant speed segments' time which are 3 & 5, total distance travelled in accelerating sections is subtracted from total distance.

$$X_{2\&6} = 20 - X_{1\&7} + X_{3\&5} \tag{2.51}$$

$$X_{2\&6} = 20 - 7.03 + 3.83 = 9.14meter \tag{2.52}$$

The time required to complete the segment is;

$$T_{2\&6} = \frac{X_{2\&6}}{V_{2\&6}} \tag{2.53}$$

$$T_{2\&6} = 1.82s \tag{2.54}$$

If we add together all the obtained and take the pick & place time as 5 seconds;

Segment no	Time (Second)
1 & 7	2.82
2 & 6	1.82
3 & 5	3.83
4	5

Table 2.6: Segment times for a cycle

When all times of the segments added up, a motion of 21.94 seconds found.

Parameters for each segment given below;

Segment no	Segment name	Segment duration [sec]	Motor torque [N-m]	Motor Speed [RPM]
1	+x acceleration	2.82	93.49	$0 \Rightarrow 3048$
2	constant speed	1.82	2.28	3048
3	+x deceleration	3.83	55.15	$3048 \Rightarrow 0$
4	Pick & place waiting time	5	0	0
5	-x acceleration	3.83	55.15	$0 \Rightarrow 3048$
6	constant speed	1.82	2.28	3048
7	-x deceleration	2.82	93.49	$3048 \Rightarrow 0$

Table 2.7: X axis Motor load parameters by segments

Calculation of RMS torque is given in 2.31. Calculated as following;

$$M_{RMS} = \sqrt{\frac{M_1^2 \cdot t_1 + M_2^2 \cdot t_2 + M_3^2 \cdot t_3 + M_4^2 \cdot t_4 + M_5^2 \cdot t_5 + M_6^2 \cdot t_6 + M_7^2 \cdot t_7}{t_{total}}} \tag{2.55}$$

$$M_{RMS} = 57.52\,Nm \tag{2.56}$$

Therefore all the required parameters are selected for motor selection in mechanical perspective. There are also options should be determined to select the motor like, cable configuration, mount orientation, encoder options etc. Also few companies offer come solutions to select and size the whole components with with in-house developed software. Siemens has "Sizer" for this purpose[24].The following motor loading table was created, by entering the parameters found, in the Siemens sizer program.

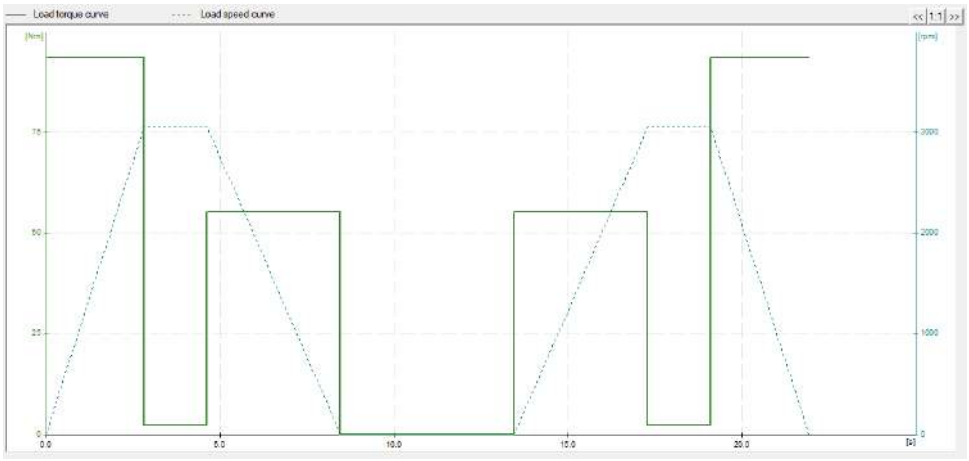

Figure 2.20: X axis motor load diagram [24]

With given parameters, software offers a motor with determined selection option. Motor selected from the Siemens Sizer given below;

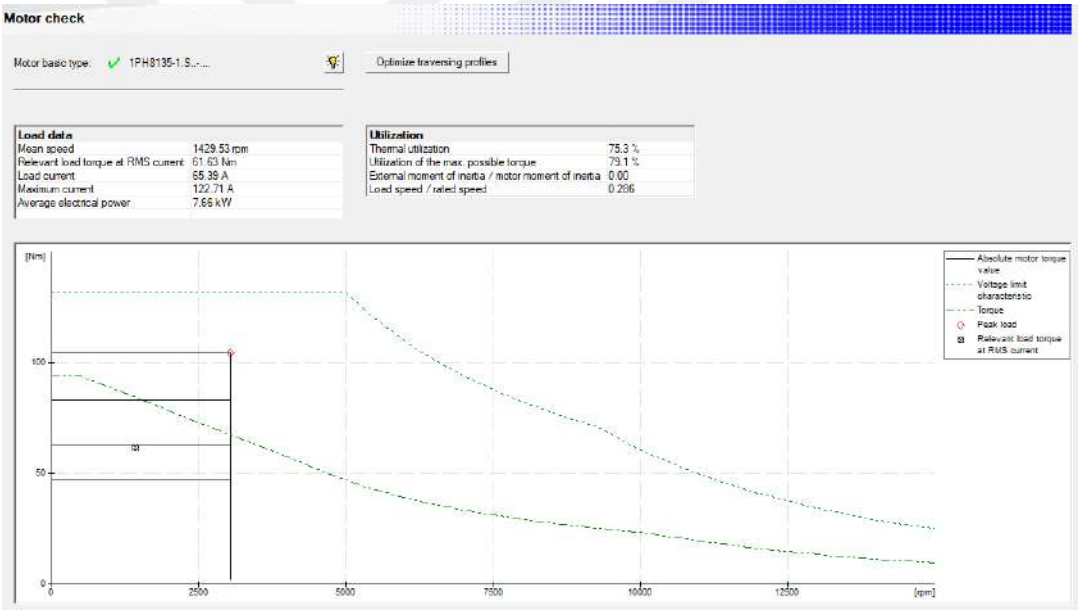

Figure 2.21: X axis motor graph [24]

2.5.1.2 RMS Torque calculation for Y axis

Y axis is the lift axis for LHD as shown in figure 1.6. In the configuration shown in 1.6 a drum carries the LHD and creates the driving force via the motor-gearbox attached to it. The same equations calculating the motor torques for x axis could be used for y axis. Instead of taking wheel diameter, the drum diameter should be taken.

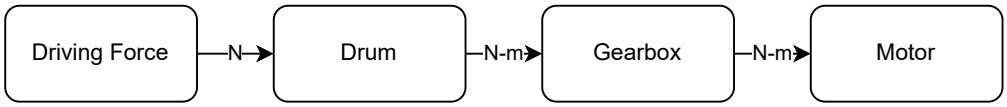

Figure 2.22: Y axis drive-train

Likewise the calculation for x axis done in 2.37, the following calculation is used for y axis.

$$\tau motor = (\frac{M \cdot a \cdot r_{drum}}{i}) / (\eta_{motor} \cdot \eta_{gearbox}) \tag{2.57}$$

Y axis also uses a gearbox with ratio 8. Thus the speed of the motor calculated as;

$$\omega_{motor} = \frac{V_y}{\pi \cdot D} \cdot 60 \cdot i \tag{2.58}$$

With equations 2.57 and 2.58 motor torque and speed requirements could be calculated for y axis. In pick&place waiting times the motor speed and torque is zero since a break, coupled to the motor, is used. Since there is no force acting on the guide wheels of the Y axis, there is no rolling resistance either.

Trapezoidal motion profile is also used for y axis as shown in 2.19. To calculate the segment durations, length of the motion in x axis is taken 7 meters. The LHD accelerates with $4\,m/s^2$ and the maximum speed is $4m/s$ as given before. LHD accelerates upward (+y) with $4\,m/s^2$ and $9.81\,m/s^2$ with downward (-y) direction. Acceleration in downward direction is done with the force of gravity, thus no load acting on the motor in that segment. Each time period of a segment is calculated with 2.45.

For segments 1 & 7;

$$T_{1\&7} = \delta V / a = 4/4 = 1s \tag{2.59}$$

Distance covered;

$$X_{1\&7} = \frac{1}{2} \cdot 4 \cdot 1^2 = 2m \tag{2.60}$$

For segments 3 & 5;

$$T_{3\&5} = \delta V/a = 4/9.81 = 0.41s \tag{2.61}$$

$$X_{1\&7} = \frac{1}{2} \cdot 4 \cdot 0.41^2 = 0.33m \tag{2.62}$$

The segments 2 & 6 required time is;

$$X_{2\&6} = totalmotiondistance - (2 \cdot X_{1\&7} + 2 \cdot X_{3\&5}) = 2.34m \tag{2.63}$$

Time required to complete the distance $X_{3\&5}$;

$$t_{2\&6} = X_{2\&6}/V_y.max = 2.34/4 = 0.58s \tag{2.64}$$

Segment no	Time (Second)
1 & 7	1
2 & 6	0.58
3 & 5	0.41
4	5

Table 2.8: Segment times for a cycle for y axis

Taking drum diameter as 200mm, torques of the segments calculated as below;

$$\tau_{motor} = (\frac{Mass \cdot a \cdot r_{drum}}{i})/(\eta_{motor} \cdot \eta_{gearbox}) \tag{2.65}$$

Motor speed for the segments calculated as below for y axis;

$$\omega_{y_{motor}} = \frac{V_y}{\pi \cdot D} \cdot 60 \cdot i \tag{2.66}$$

Calculation of RMS torque is given in 2.31. Calculated as following;

Segment no	Segment name	Segment duration [sec]	Motor torque [N-m]	Motor Speed [RPM]
1	+y acceleration	1	57.38	$0 \Rightarrow 3055$
2	constant speed	0.58	40.76	3055
3	+y deceleration	0.41	0	$3055 \Rightarrow 0$
4	Pick & place waiting time	5	0	0
5	-y acceleration	0.41	0	$0 \Rightarrow 3055$
6	constant speed	0.58	40.76	3055
7	-y deceleration	1	57.38	$3055 \Rightarrow 0$

Table 2.9: Y Axis motor load parameters by segments

$$M_{RMS} = \sqrt{\frac{M_1^2 \cdot T_1 + M_2^2 \cdot T_2 + M_3^2 \cdot T_3 + M_4^2 \cdot T_4 + M_5^2 \cdot T_5 + M_6^2 \cdot T_6 + M_7^2 \cdot T_7}{T_{total}}} \tag{2.67}$$

$$M_{RMS} = \sqrt{\frac{57.38^2 \cdot 1 + 40.76^2 \cdot 0.58 + 40.76^2 \cdot 0.58 + 57.38^2 \cdot 1}{8.98}} = 30.78Nm \tag{2.68}$$

The following motor loading table was created, by entering the parameters found, in the Siemens sizer program.

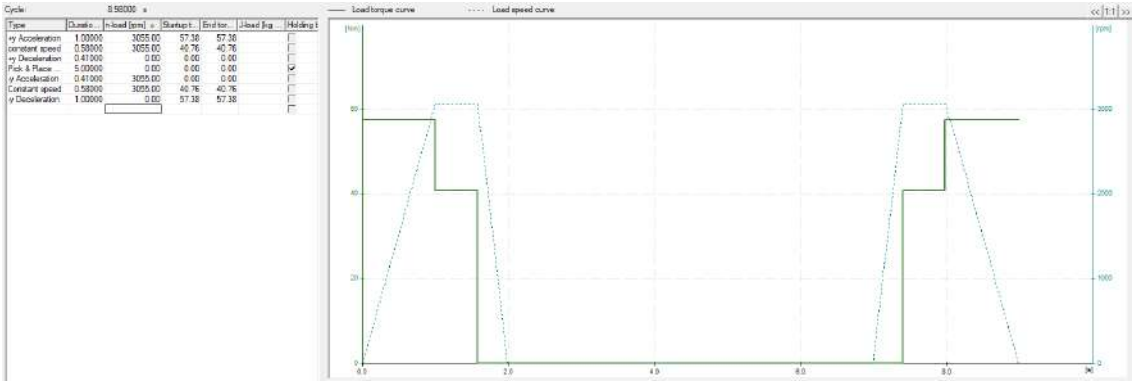

Figure 2.23: Y axis motor load diagram [24]

With given parameters, software offers a motor with determined selection option. Motor selected from the Siemens Sizer given below;

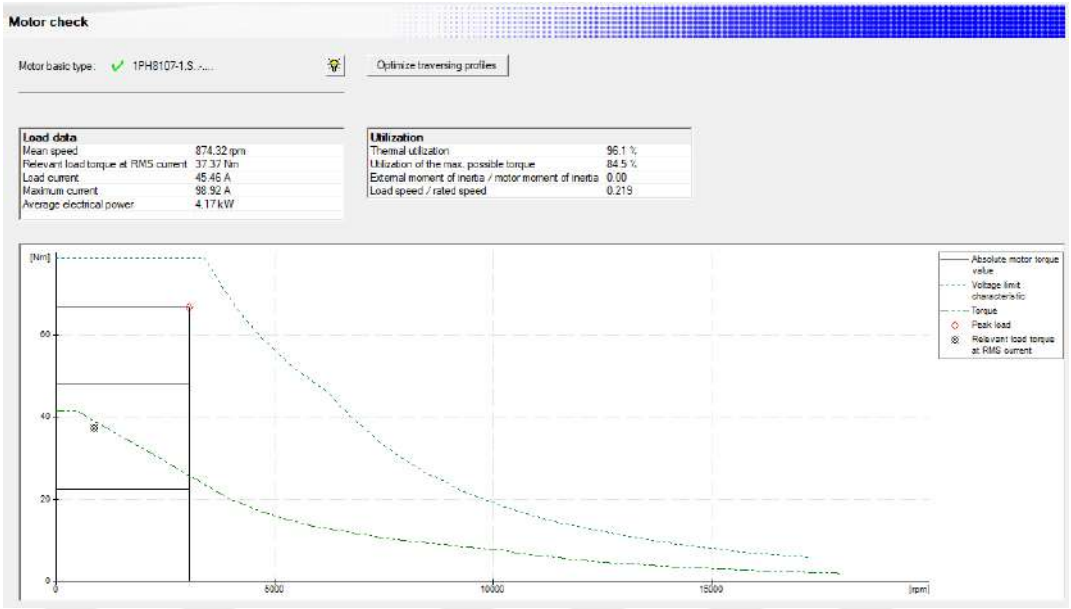

Figure 2.24: Y axis motor graph [24]

2.6 Safety Equipment and Sensors

There are several safety related equipment and configuration of some mechanical components must be used, in order to operate the stacker crane safely. Although the most important security measure is to program the crane to operate in predetermined limitations, there are human errors, unforeseen mechanical problems and software errors. Suggested safety equipment for stacker cranes given below.

- Safety brakes on motors: Motors in stacker crane are equipped with safety related brakes. The brake needs energy to keep open at any time so that, if there is a power cut off or interruption to the system, motor brake engages and slows down the axis that it's connected to.
- 2-D scanner: A 2 dimensional laser scanner is placed on the mast and it checks that the gap between the tower and the racks is blocked by any object. This ensures that the stacker crane can safely travel in x axis (aisle axis) without a risk to trip an object and make it fall.
- Safety shock absorbers: Safety shock absorbers are used to stop an

incorrectly operated or out of control stacker crane. They are positioned at the end of each axis and selected according to the energy that stacker crane is assumed to have if an impact occurs.

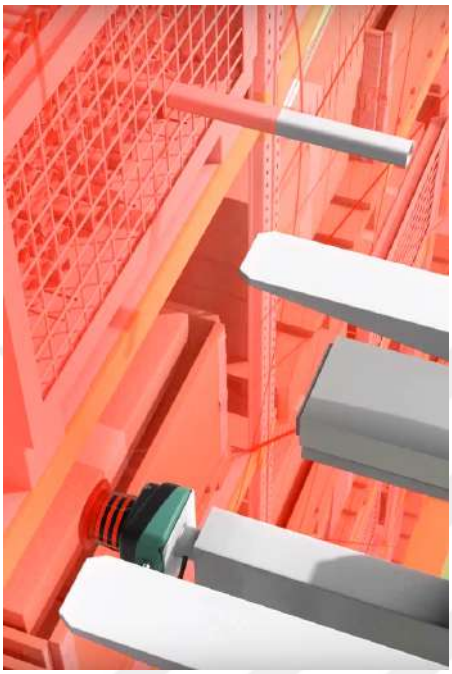

(a) 2-D Scanner [16]



(b) Safety Shock Absorber[1]

Figure 2.25: Safety Equipments

The sensors placed on the stacker crane provide the system with the status of the system. Since a stacker crane is a system that travels it is necessary to connect the system to the main PLC (Programmable Logic Controller) that is feeding the information that what should stacker crane do next. There are also other miscellaneous sensors, that help the stacker crane work more robust will be mentioned below. The sensors used in the stacker crane given below.

- Positioning sensors: Even though all the motors in stacker crane has encoders integrated in it, it can drift over time and gives incorrect position. To avoid this, positioning sensors are used in ASRS operations along with the positioning code tapes placed on the axes. To read this

position codes, cameras are added to each individual axis. So that the stacker crane will not lose its position even after a restart.

- Optical data coupler: To transfer information to base of ASRS to the stacker crane is crucial. Although this can be done with a cable drag chain, since the corridors are very long is a common situation in ASRS systems, wireless communication options are preferred in such operations. Wireless communication is provided by the transceiver standing at the beginning of the corridor and on the stacker crane.
- Vision Sensor: This sensor helps the stacker crane position itself more precise. The camera positioned on LHD, detects the position of an index hole that is on the shelves. The main use of this sensor is to accurately record the positions of all shelves during initial setup.



(a) Vision Sensor (b) Code tape (c) Optical Data Coupler

Figure 2.26: Miscellaneous Sensors

3. Control of Stacker Crane

Stacker crane structure is exposed to vibration during crane movement. Detecting and reducing the vibration of the stacker crane is critical due to safety and time management reasons. LHD cannot extend before the vibrations of the stacker crane falls below a certain level. In this chapter a mathematical model for the stacker crane and a control algorithm will be presented.

3.1 Mathematical Model Derivation

An equivalent mass at the tip of the mast and an equivalent stiffness for the system has been found in chapter 2.12. Together with the reduced masses found, the stacker crane can be reduced to a double mass spring system in order to derive a mathematical model.

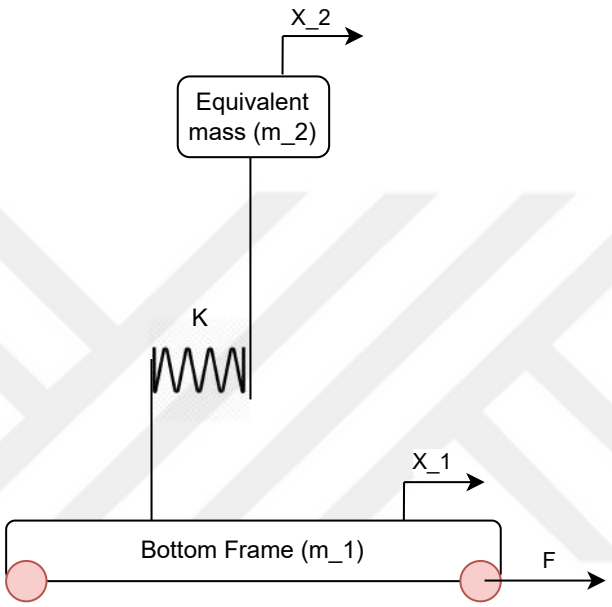

Figure 3.1: Motion system of the stacker crane with equivalent mass and spring

Position of the bottom frame is x_1 and position of the tip of the crane is x_2. There is only a spring between two masses which is derived in 2.6. System dynamics are given in the equations below. $x_1 > x_2$ is assumed.

$$m_1\ddot{x}_1 = -k(x_1 - x_2) + F \tag{3.1}$$

$$m_2\ddot{x}_2 = k(x_1 - x_2) \tag{3.2}$$

$$\ddot{x}_1 = \frac{-k(x_1 - x_2)}{m_1} + \frac{F}{m_1} \tag{3.3}$$

$$\ddot{x}_2 = \frac{k(x_1 - x_2)}{m_2} \tag{3.4}$$

3.2 Natural Frequency of Stacker Crane

If the equations in 3.2 are rearranged, the following dynamic equilibrium equations are obtained.

$$m_1\ddot{x}_1 + k(x_1 - x_2) = 0 \tag{3.5}$$

$$m_2\ddot{x}_2 - k(x_1 - x_2) = 0 \tag{3.6}$$

These equations with free vibrations are solved for displacements by substituting;

$$x_1 = a_1\, sin(\omega t - \alpha) \tag{3.7}$$

$$x_2 = a_2\, sin(\omega t - \alpha) \tag{3.8}$$

To derive the accelerations, displacements are derived twice. Therefore, the following equations are obtained.

$$\ddot{x}_1 = -a_1\omega^2\, sin(\omega t - \alpha) \tag{3.9}$$

$$\ddot{x}_2 = -a_2\omega^2\, sin(\omega t - \alpha) \tag{3.10}$$

If the equations are written as a matrix, the following matrix equations are obtained.

$$\begin{bmatrix} k - m_1\omega^2 & -k \\ -k & k - m_2\omega^2 \end{bmatrix} \begin{bmatrix} a_1 \\ a_2 \end{bmatrix} = \begin{bmatrix} 0 \\ 0 \end{bmatrix} \tag{3.11}$$

For a nontrivial solution determinant of the coefficients must be equal to zero.

$$\begin{vmatrix} k - m_1\omega^2 & -k \\ -k & k - m_2\omega^2 \end{vmatrix} = 0 \tag{3.12}$$

$$m_1 m_2 \omega^4 - \omega^2(m_1 k + m_2 k) = 0 \tag{3.13}$$

Since the general equation for the is found natural frequency of the stacker crane could be found via implementing the values of stacker crane. m_1 is determined to be $1200kg$ and m_2 is the weight of the lumped mass. Lumped mass includes the weight of the LHD, payload and the reduced weight of the mast. The natural frequency of the system changes with the change of m_2.

Since the stacker crane carrying different types of load, weight of the mass m_2 depends on whether the LHD carries a load or not or the weight of the load it carries. As the weight of the load varies between $0 - 100kg$, the weight of the LHD varies between 246 to $346kg$.

There is a single root for the function 3.13 that is nontrivial. Natural frequency of the stacker crane found between the range stated below.

$$\omega = 27.9 \; - \; 31.98\, Rad/sec \tag{3.14}$$

3.3 State Space Representation of the Stacker Crane

With the dynamics of the system is found in 3.4 the state space representation of the stacker crane can be written like following.

$$\dot{x}(t) = Ax(t) + Bu(x) \tag{3.15}$$

$$y(t) = Cx(t) \tag{3.16}$$

$$\begin{bmatrix} \dot{x}_1 \\ \dot{x}_2 \\ \ddot{x}_1 \\ \ddot{x}_2 \end{bmatrix} = \begin{bmatrix} 0 & 0 & 1 & 0 \\ 0 & 0 & 0 & 1 \\ -\frac{k}{m_1} & \frac{k}{m_1} & 0 & 0 \\ \frac{k}{m_2} & -\frac{k}{m_2} & 0 & 0 \end{bmatrix} \begin{bmatrix} x_1 \\ x_2 \\ \dot{x}_1 \\ \dot{x}_2 \end{bmatrix} + \begin{bmatrix} 0 \\ 0 \\ \frac{1}{m_1} \\ 0 \end{bmatrix} F \tag{3.17}$$

$$y(t) = \begin{bmatrix} 1 & 0 & 0 & 0 \end{bmatrix} \begin{bmatrix} x_1 \\ x_2 \\ \dot{x}_1 \\ \dot{x}_2 \end{bmatrix} \tag{3.18}$$

A matrix represents the system dynamics, B matrix is the input and C matrix is measurements. Only input u(t) to the system is generated by the horizontal axis motor which creates the force F via gearbox and the drive wheel. Measured output of the system is the position of bottom frame with a positioning sensor.

3.4 Trajectory Planning

Stacker crane consist mainly consists of 3 axis linear motion. Crane moving along the corridor, vertical movement of LHD module and pick and place motion of it. There are also other axes like the gripper and a conveyor in LHD. The axis covered in this thesis is the corridor axis called the x-axis which creates the vibrations in the mast. Whenever a new command is given to the stacker crane, first the trajectories according to the command should be generated. Then the stacker crane moves accordingly.

While moving within a trajectory, computer and the hardware of the system controls and generates the feed-forward command and feedback control. As stated in 3.1 stacker crane is reduced to a two point mass. Controlling the stacker crane is critical for two main reasons. First to reduce the vibration of the LHD module in order to reduce settling time and for limiting actuator effort to limit motor size.

Trapezoidal trajectory shown in 2.19; this trajectory assumes that the jerk and acceleration is infinite, thus there are sharp corners in trajectory that can lead vibrations in the stacker crane. With trajectory smoothing (shaping) acceleration and velocity bounds are used in order to create s-shaped, symmetrical trajectory.

To achieve that being mentioned, trajectory smoothing, feed-forward force generation is used with 4th order system in this research. To generate a 4th order force feed-forward signal, the trajectory of the system should be generated starting from jerk command. Jerk is generally bounded by the rise time of the power amplifier (motor controller). Symmetrical trajectory consists of four phases. Constant derivative of jerk, Constant jerk, constant acceleration and constant speed. Horizontal axis being time and vertical axes represents the parameters given in the headline of the graph accordingly. Bounds of the given sample trajectory is stated below.

Derivative of jerk	500 $[m/s^4]$
Jerk	30 $[m/s^3]$
Acceleration	3 $[m/s^2]$
Speed	5 $[m/s]$

Table 3.1: Bounds on parameters for sample trajectory

A sample position command with $10\,meter$ displacement of stacker crane in x axis is given in figure 3.2.

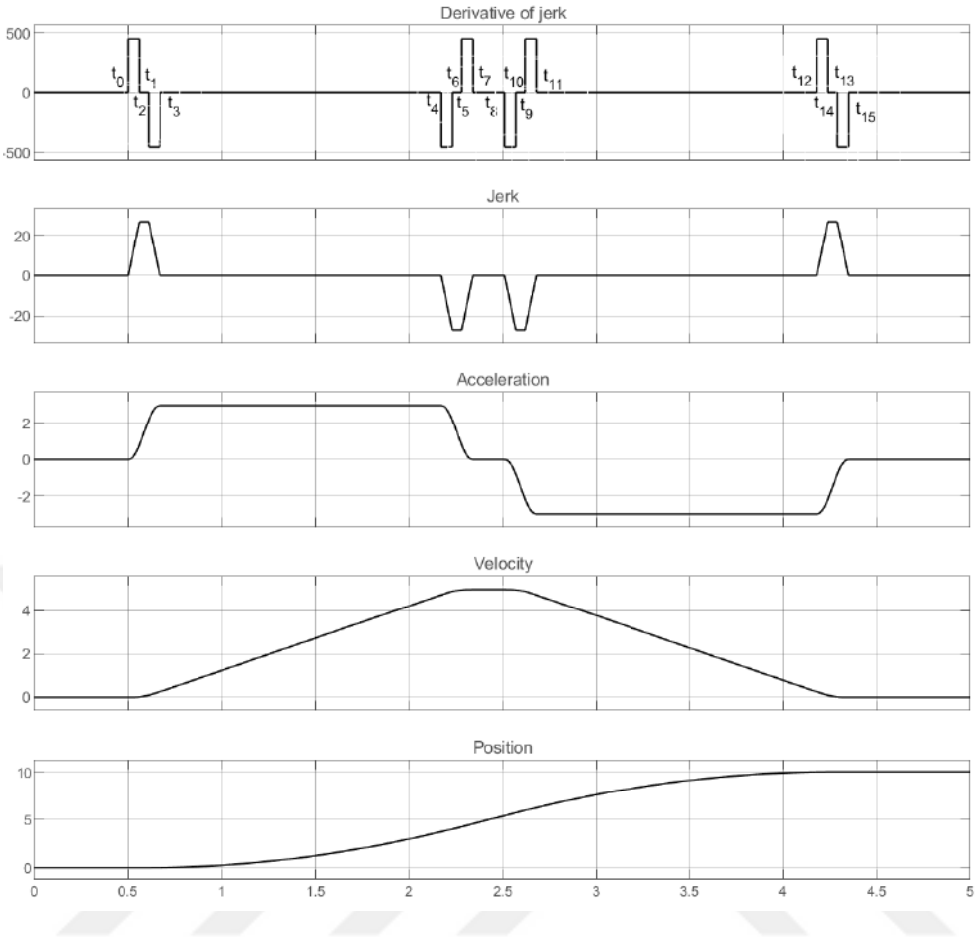

Figure 3.2: Trajectory profiles for 4th order system

Time intervals are marked on the figure, it represents the time instance that the derivative of jerk changes. Using bounds on the parameters one can calculate, jerk, acceleration, velocity and distance travelled for each section. In this thesis the library created by [10] used in Matlab/Simulink in order to generate the desired trajectory for given parameters and find the required feed-forward force for the system.

Parameters for the first time interval $t_0 - t_1$ calculated as follows;

$$j(t) = d_0 + j_0 \tag{3.19}$$

$$a(t) = \frac{1}{2}d_0t^2 + j_0t + a_0 \tag{3.20}$$

$$v(t) = \frac{1}{6}d_0t^3 + \frac{1}{2}j_0t^2 + a_0t + v_0 \tag{3.21}$$

$$x(t) = \frac{1}{24}d_0t^4 + \frac{1}{6}j_0t^3 + a_0t^2 + v_0t + x_0 \tag{3.22}$$

Like the equations given above, parameters for each segment can be calculated. Calculation for each segment and more detail for the trajectory planning could be found in [10].

3.5 Feed-Forward Force Calculation

Feed-forward control is used in systems that are the disturbances of the systems are known in before acting on the system. Setpoint of the accelerations in stacker crane is known before the system starts its operation. These intervals are defined in section 3.4.

To obtain a desired trajectory with minimal settling time for LHD, feedforward control is used in conjuction with feedback control. Since trajectory generation algorithm is determined in previous section 3.4, feedforward force should be calculated in order to get an input for the induction motor accoupled to the bottom frame stated as the mass m_1 in figure 3.1. In conclusion while the setpoints of the trajectory is known, there will be a feedforward force calculated in order to follow the desired trajectory, hence reducing the settling time and following error of the LHD which symbolized as m_2. To calculate the feed-forward force in question one must determine the transfer function from lineer force acting on the bottom frame m_1 to the position of lumped mass m_2.

Using equations 3.2 transfer function from input force F to x_2 is found

with Laplace transform of the equations.

$$m_1 x_1 s^2 = -k(x_1 - x_2) + F \tag{3.23}$$

$$m_2 x_2 s^2 = k(x_1 - x_2) \tag{3.24}$$

$$x_1 = \frac{m_2 x_2 s^2 + k x_2}{k} \tag{3.25}$$

Using x_1 found in 3.24 the transfer function from F to x_2 will be;

$$\frac{F}{x_2} = \frac{m_1 m_2 \cdot s^4 + (m_1 + m_2) k \cdot s}{k} \tag{3.26}$$

With this the force required for the fourth order trajectory can be calculated as following.

$$F = \frac{1}{k} \cdot \{m_1 m_2 \cdot s^4 + (m_1 + m_2) k \cdot s\} \cdot x_2 \tag{3.27}$$

With derivatives of the x_2 corresponds to the powers of s term. Derivatives of x_2 being speed, acceleration and jerk. Block diagram of using feed-forward for the stacker crane given in 3.3.

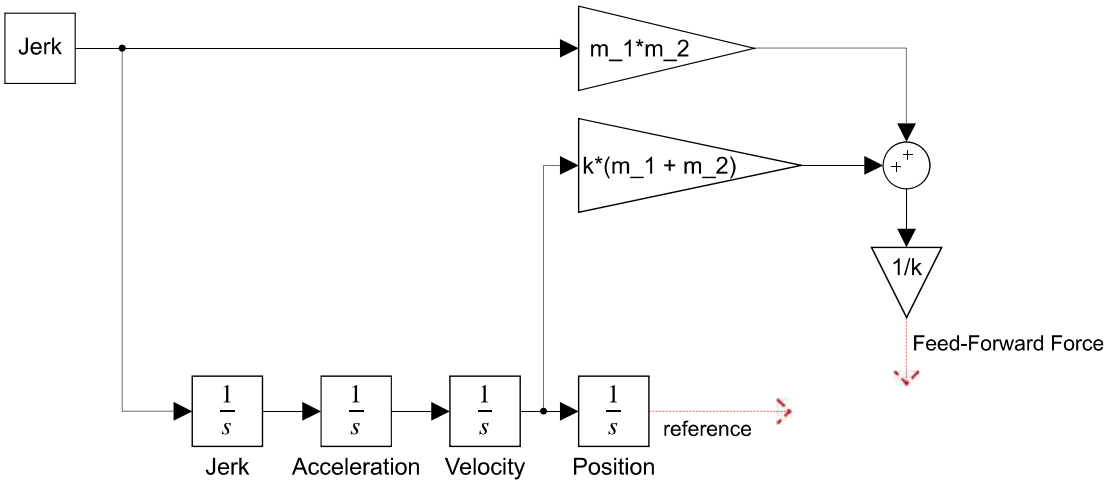

Figure 3.3: Feed-Forward force block diagram

3.6 Control Approach

With all being written in this thesis the control approach to the real machinery should be applied and numerical results are extracted from this simulation. In practical application with the product being delivered induction motor will be used and it is controlled with a PLC (programmable logic controller). Stacker crane is given a command to go to a place and pick up or drop a load. This command is given by a higher level program and the PLC on the stacker crane should process this command into a meaning-full set of signals.

Schematics of the flow of the process is given below.

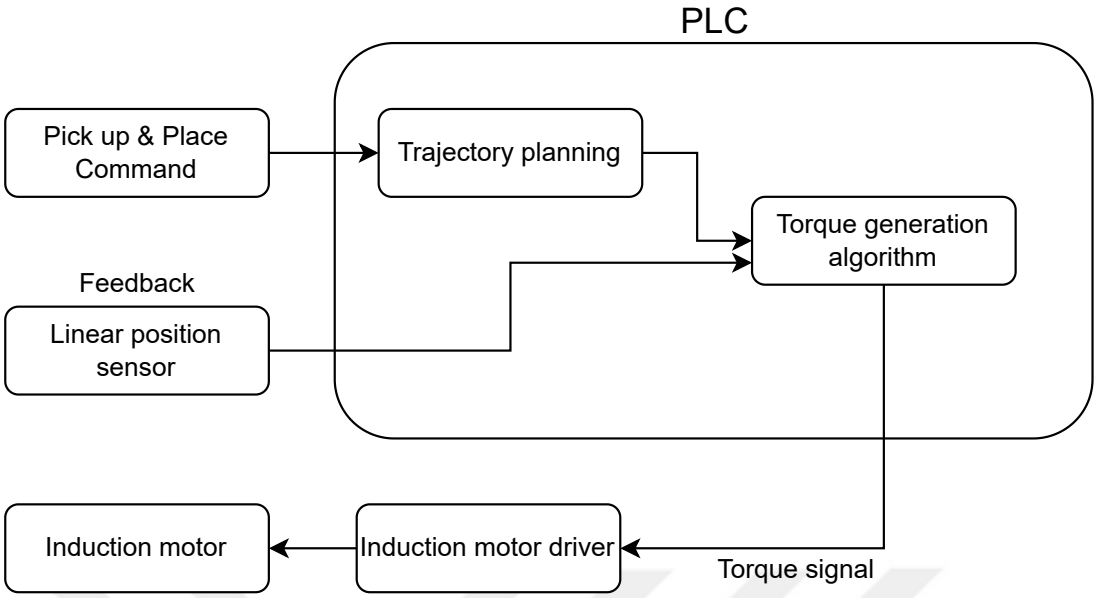

Figure 3.4: Control flow schematic

Since this thesis constitutes the control part of a product made in a company, it is aimed to match the company's conventional control methods. For this reason, the induction motor was modeled using the FOC (field oriented control) (commonly called AC3 motor drive) [13] control block in the Simulink model and the signals created were the input of this motor. FOC is selected because its ability to fast dynamic response.

Induction motors can be used in either in torque command mode or speed command mode. An induction motor driver generally capable of driving the motor in both modes but it needs to be reset in between the modes. This is unacceptable in dynamic systems.

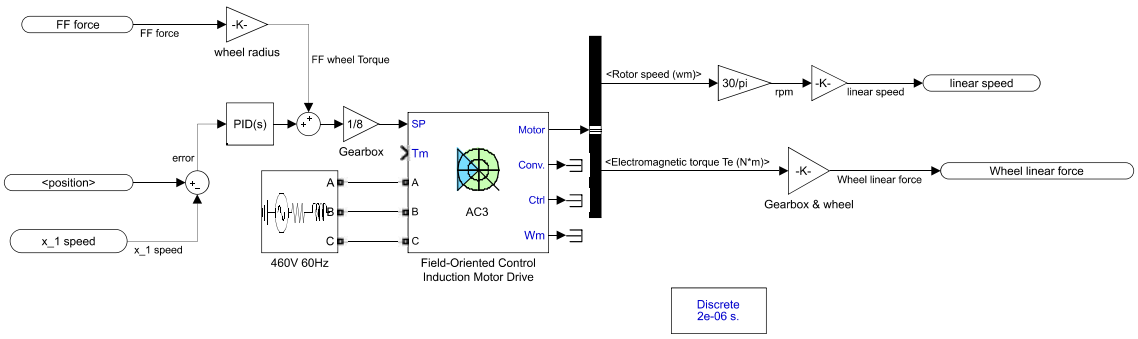

Figure 3.5: Induction motor simulink model

Induction motor control model is given in 3.5. In this work to be done induction motor is driven in torque mode in inner loop and there is an outer loop which contains the speed error of the plant which transforms this speed error with PID block to an input to the induction motor. FOC control block is used with torque set-point and 460V 60Hz voltage supply. Input signal given to the motor consist of 2 main parts. First being the pre-calculated system force converted into motor torque by multiplying it with gain block which contains wheel radius as the multiplier and the second part is feedback control which calculates the error by subtracting plant velocity $\dot{x}_1$ from reference velocity taken from continuous time feed-forward [10] block.

As shown in 3.4, PLC is the computational machine in the system which also controls the communication between components. Pick & Place command is given by a higher system like a WMS (warehouse management system), trajectory is generated and with torque generation algorithm a torque signal is created for induction motor driver. Any error caused by the uncertainties in the stacker crane could be corrected with the linear position sensor which is fixed in the bottom frame. So the linear position sensor is used as a feedback mechanism in this system.

Command to the stacker crane machine is written in the blocks which

are created by [10]. Block is given in the figure 3.6. For an example $3 meter$ command parameters are defined in this block.

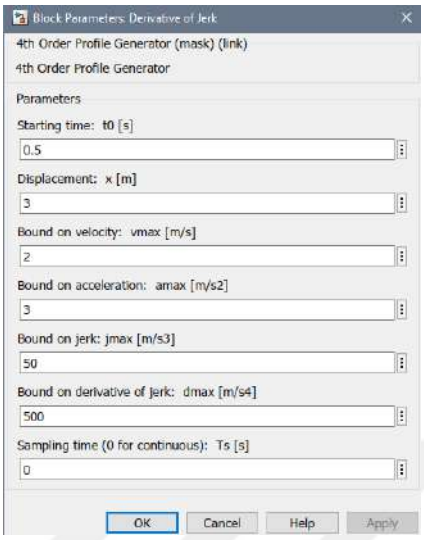

Figure 3.6: Profile Generator Block [10]

The simulink model that simulates the entire system is shown in the figure 3.7. For given parameters to the profile generation block, the block creates a derivative of the jerk command, this command processed by the feed-forward block and it creates feed-forward force, reference position to be fed to the induction motor. Additionally derivative of jerk, jerk, acceleration and velocity commands are created in this block but it is not used in this simulation. Feed-forward force and position command is given to the induction motor subsystem. Subsystem is defined beforehand in this chapter and it creates linear speed output and wheel linear force as an output. Wheel linear force is fed to the plant which was defined in chapter 3.3. Only the x_1 position is fed back to the system as it being the only parameter that being measured. Other parameters created for to understand how the whole system is behaving under given force command.

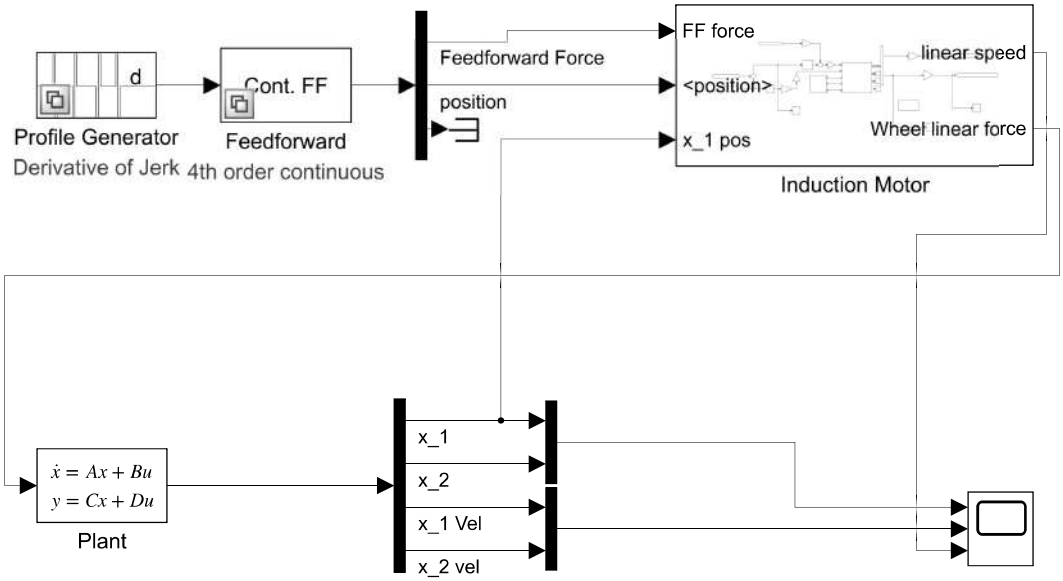

Figure 3.7: Stacker crane simulink model

3.7 Notch Filter Design

Control commands are created for perfectly designed stacker crane model, but in reality there are some flaws for the model like differences in material properties, manufacturing defects, friction and guide rail misalignment. One or more of these errors can create a resonant frequency in the stacker crane. It crucial to not to let this resonant frequency goes into the controller which then commanding the actuator, this might lead excitation of the system more.

Notch filter is used for this kind of situations in mechanical systems in order to filter out the frequencies feed into to controller by attenuating the signal frequencies that overlaps with the mechanical system's natural frequency. Notch filter for the stacker crane designed in Matlab "control system designer".

Notch filter is designed to be cancelling out the frequencies around the natural frequency of stacker, which stated in 3.2. Altough the natural fre-

quency of the stacker crane is changing depending on whether there is a payload on it or not and the weight of the payload, bandwidth of the notch filter is capable of covering those natural frequency changes. Those frequencies are found to be changing between 27.9 Rad/sec to 31.2 Rad/sec with the changing weight of the payload. The peak filtering frequency of the notch filter should be set to the most used payload weight and the bandwidth should cover the range from lowest natural frequency to highest. For the stacker crane designed in this study peak filtering frequency is set to 29.5 Rad/sec, which is the average of the heaviest and lightest payload and the banwidth is set to the range of the change in natural frequency.

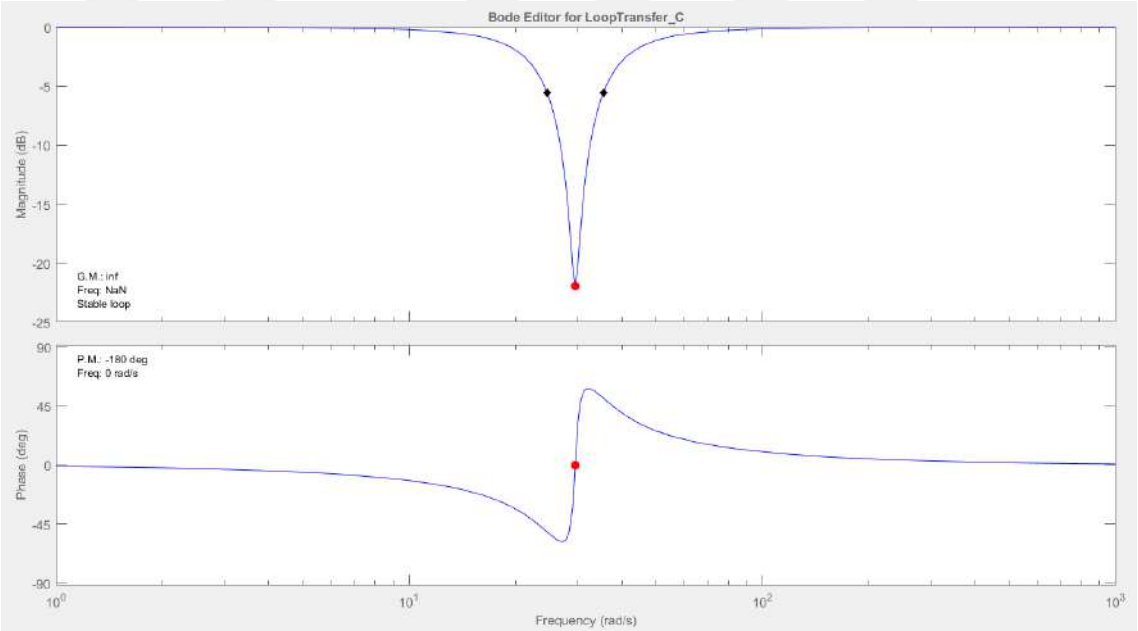

Figure 3.8: Bode plot of the notch filter

Notch filter bandwitdh is selected regarding to the changing range for the stacker crane. It attenuates to frequencies ranging from 25 Rad/sec to 35 Rad/sec. This range of 10 Rad/sec was obtained by adding a tolerance on the previously found natural frequencies. Notch filter attenuating gain set to 22 dB to cancel out the gains in in the resonant requency. this value will attenuate the input signal by 0.07. If this value does not limit the

resonance in practical application, a higher coefficient attenuating gain will have to be used.

Transfer function of notch filter is given below;

$$\frac{s^2 + 1.402s + 870.3}{s^2 + 17.65s + 870.2} \tag{3.28}$$

Notch filter is tested with an impulse of power $10N$. Simulink model is given below. A notch filter is integrated right before the controller in order to filter out the signals that has the frequency same as the natural frequency.

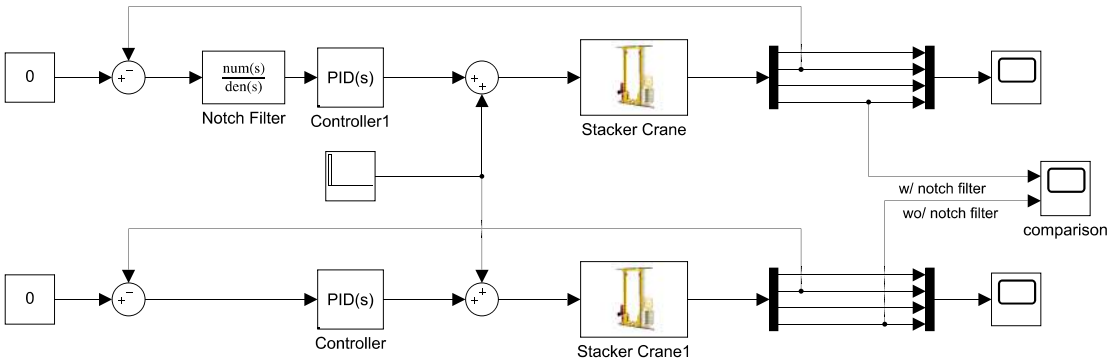

Figure 3.9: Notch filter test in simulink

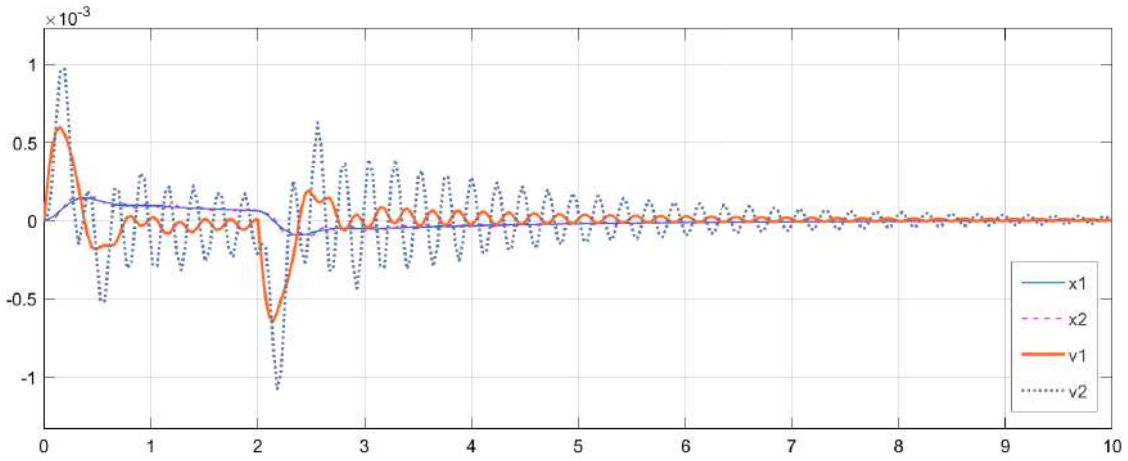

Figure 3.10: System response of the upper system in figure 3.9 with notch filter

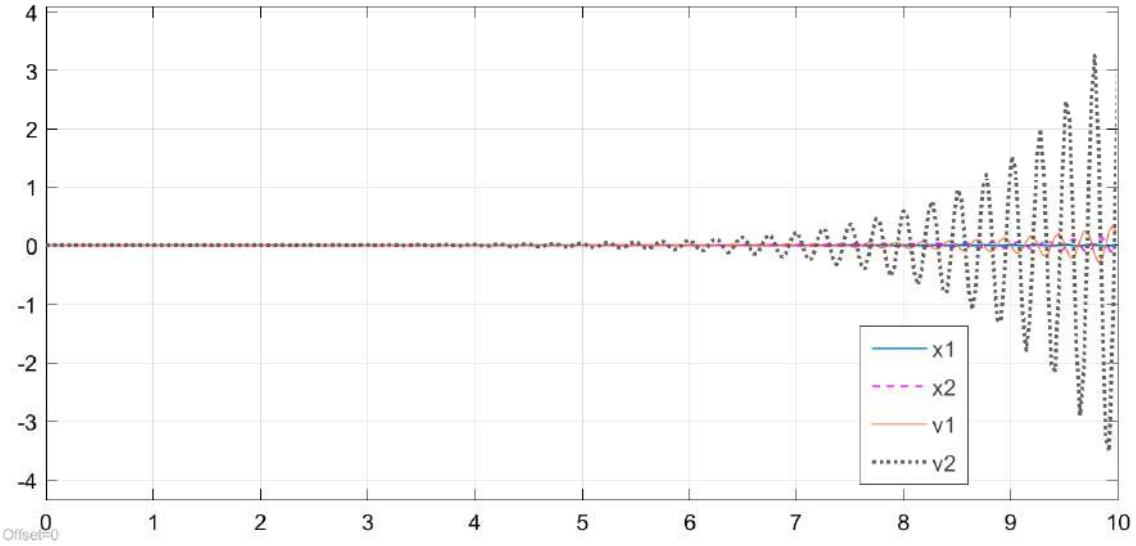

Figure 3.11: System response of the lower system in figure 3.9 without notch filter

Figures are plotted for the range of the varying natural frequencies of the stacker crane and the results of the performance of the system is given in the figures. Since the bandwith of the notch filter is designed to filter out the varying natural frequencies of the system results are the same for the stacker whether if it is carrying a payload or not. The designed notch filter prevented the system from vibrating at resonant frequencies.

4. Simulation Results

Simulation of the stacker crane is done in simulink and the results are obtained via scope blocks. For comparison different data collected by the scope blocks in simulink is used apart from the figure 3.7. The simulated trajectory parameters are defined in figure 3.6.

For the sample trajectory and feed-forward force acceleration, position and speed of the LHD is given. As seen from the figure 4.1 system has a trapezoidal speed profile and follows the given reference in a margin. Performance of the system is determined by the time it has to spend to

move the LHD in determined position with $\pm 2\,mm$. From figure 4.2 it is seen that the LHD has much lower error following the reference trajectory with the feed-forward force.

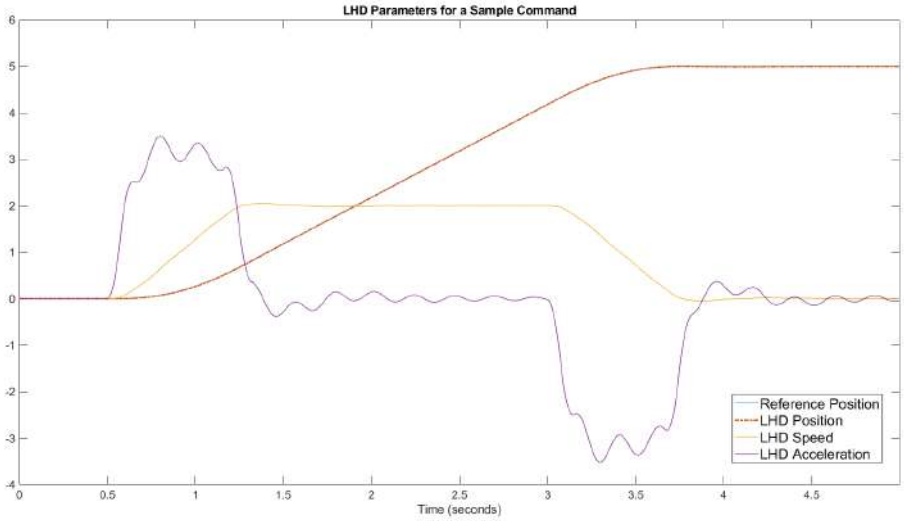

Figure 4.1: LHD parameters for sample trajectory

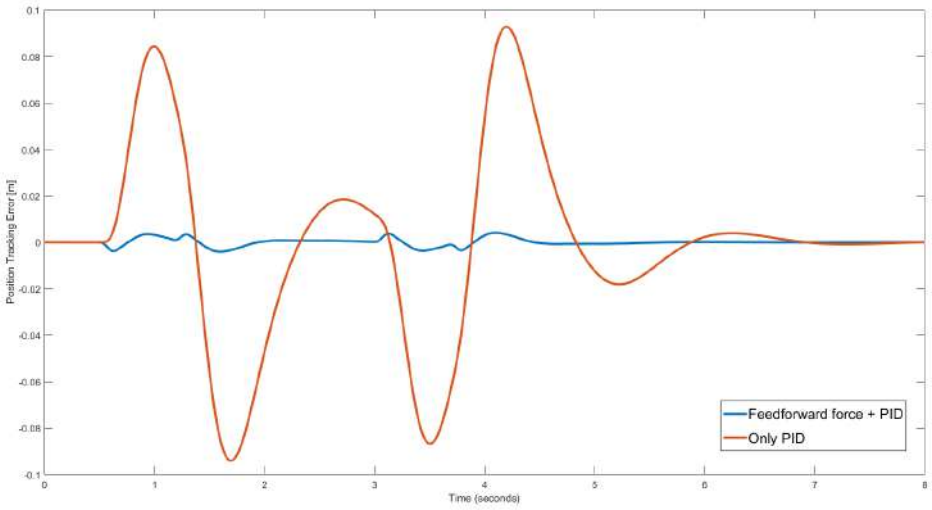

Figure 4.2: Trajectory follow error with and without feed-forward force

5. Conclusion

Through the work done in this thesis, a stacker crane machine's main elements are designed accordingly and a control algorithm is created for industrial stacker crane machines. An originality of this thesis is that an induction motor is implemented in the control algorithm and defined how the motor should be used in industrial control algorithms with PLC and induction motor drivers.

REFERENCES

[1] ACE. Safety shock absorbers sdh38 to sdh63. https://www.ace-ace.com/com/products/safety-products/safety-shock-absorbers/sdh38-to-sdh63.html. Accessed: 2022-03/06.

[2] Y. A. Bozer and J. A. White. Travel-time models for automated storage/retrieval systems. *IIE Transactions*, 16(4):329–338, 1984.

[3] J. S. Dave Lippert. https://www.hamiltoncaster.com/Blog/EntryId/222/Rolling-Resistance-and-Industrial-Wheels. Accessed: 2022-02-12.

[4] FEM. Basis of calculations for SIR machines, tolerances, deformations and clearances in automatic small parts warehouses (not silo design). Standard, FEM, 2001.

[5] A. Filippatos, M. Dannemann, D. Wohlfahrt, N. Modler, and T. Schmidt. Design of a highly damped fibre-reinforced lightweight mast for automated storage systems in logistics. 07 2016.

[6] W. Hausman, L. Schwarz, and S. Graves. Optimal storage assignment in automatic warehousing systems. *Management Science*, 22:629–638, 02 1976.

[7] H. HWANG and S. B. LEE. Travel-time models considering the operating characteristics of the storage and retrieval machine. *International Journal of Production Research*, 28(10):1779–1789, 1990.

[8] H.-Y. Jiao, F. Li, Z.-Y. Jiang, Y. Li, and Z.-P. Yu. Periodic topology optimization of a stacker crane. *IEEE Access*, PP:1–1, 12 2019.

[9] R. Kriger. Rose kriger heavy duty profiles. https://www.rk-rose-krieger.com/english/. Accessed: 2022-04-09.

[10] P. Lambrechts, M. Boerlage, and M. Steinbuch. Trajectory planning and feedforward design for electromechanical motion systems. *Control Engineering Practice*, 13(2):145–157.

[11] A. Macchelli and C. Melchiorri. Modeling and control of the timoshenko beam. the distributed port hamiltonian approach. *SIAM J. Control and Optimization*, 43:743–767, 01 2004.

[12] W. L. Mario Paz. *Structural Dynamics Theory and Computation*. SPRINGER SCIENCE+BUSINESS MEDIA, LLC, 5 edition, 2005.

[13] MathWorks. Field-oriented control induction motor drive. https://www.mathworks.com/help/physmod/sps/powersys/ref/fieldorientedcontrolinductionmotordrive.html. Accessed: 2022-05-24.

[14] Mecalux. Stacker cranes for boxes. https://www.mecalux.com/automated-warehouses-for-boxes/stacker-cranes-for-boxes. Accessed: 2022-01-24.

[15] Mias. Stacker cranes from the akl series. https://mias-group.com/en/stacker-cranes-as-rs/miniload-akl-series/. Accessed: 2022-02-05.

[16] Pepperl+Fuchs. R2000 series detection laser. https://www.pepperl-fuchs.com/global/en/R2000_Detection_laser_scanner.htm. Accessed: 2022-03/06.

[17] B. A. PETERS, J. S. SMITH, and T. S. HALE. Closed form models for determining the optimal dwell point location in automated storage and retrieval systems. *International Journal of Production Research*, 34(6):1757–1771, 1996.

[18] B. Post, A. Mariuzza, W. Book, and W. Singhose. Flatness-based control of flexible motion systems. volume 1, 01 2011.

[19] H. Rotomat®. Hänel rotomat® industrial vertical carousels. https://www.mazzellacompanies.com/solutions/product/hanel-rotomat-industrial-vertical-carousels/. Accessed: 2022-01-24.

[20] K. Ruehrdanz. As/rs: A history of innovation. https://blog.dematic.com/en-us/ASRS-A-History-of-Innovation/. Accessed: 2022-01-24.

[21] M. Sasaki, T. Shimizu, K. Ikai, and S. Ito. Stabilized controller design for a flexible stacker crane. In *SICE Annual Conference 2007*, pages 874–878, 2007.

[22] Siemens. General technical specifications for simotics motors for cranes. https://mall.industry.siemens.com/mall/en/WW/Catalog/Products/10234350#. Accessed: 2022-02-10.

[23] Siemens. Nx 10.

[24] Siemens. Sizer for siemens drives engineering tool (integrated in the tia selection tool). https://mall.industry.siemens.com/mall/tr/tr/Catalog/Product/6SL3070-0AA00-0AG0. Accessed: 2022-02-14.

[25] M. Staudecker, K. Schlacher, and R. Hansl. Passivity based control and time optimal trajectory planning of a single mast stacker crane. *IFAC Proceedings Volumes*, 41(2):875–880, 2008. 17th IFAC World Congress.

[26] B. H. Tongue. *Principles of Vibration (2nd Edition)*. Oxford University Press, 2002.

[27] M. Vasili, S. Tang, and M. Vasili. Automated storage and retrieval systems: A review on travel time models and control policies. *Warehousing in the Global Supply Chain*, pages 159–209, 02 2014.

[28] Vulkoprin. Vulkoprin. `https://www.vulkoprin.be/en/`. Accessed: 2022-04-09.

[29] H. Yoon, S. Y. Chung, H. Kang, and M. Hwang. Trapezoidal motion profile to suppress residual vibration of flexible object moved by robot. *Electronics*, 8:30, 01 2019.

SUMMARY

As a graduate of Yildiz Technical University and an enthusiast engineer, I am an excellent anticipator of problems and thus a passionate engineer to find the best solutions to those problems within the engineering markets. Through my past internships and industrial employment experiences, I excelled in utilizing all possible opportunities towards my personal development. I am seeking a position as an engineer where my ability to offer efficiency through analytical thinking and innovation can be utilized fully.

Ozan Erdem DEMİREL

Mechanical Engineer

EXPERIENCE

Mechanical Design Engineer in R&D department
(November 2017 - Present)

Altınay Robot Technologies - İstanbul, Türkiye

- Modelling robust and precise robotic systems with several CAE and FEM programs.
- Actuator design and selection for complex, dynamic systems.
- Selecting optimal parts for systems with making contacts with suppliers.
- Creating technical drawings with GD&T.
- Design and control of a stacker crane (Automated storage and retrieval system).
- Mechanical design and control for industrial indoor AMR.(Autonomous Mobile Robot)

Laboratory Assistant in chair of dynamics and mechatronics
(August 2017-October 2017)

Paderborn University - Paderborn, Germany

- Analyzed state of art sonotrode horn designs with ansys fluent for cleaning processes.
- Conducted heat analysis with ansys fluent for maintaining safe heat level for sonotrode.
- Conducted more than 500 cycle tests and created a reporting system in matlab on the developed multi-dimensional wire bonding system.
- Facilitated the advancement of brushless DC motor designs by administering torque and magnetism analysis.

EDUCATION

M.Sc. Mechanical Engineering
(2019-)*

Marmara University - İstanbul, Türkiye
Thesis: Design and control of a stacker crane

- Design methodology
- Optimization of gear mechanism
- Vibration analysis methods
- System dynamics and control

B.Sc. Mechanical Engineer
(2013-2017)

Yıldız Technical University - İstanbul, Türkiye

- Hydraulics and Pneumatics
- Advanced Calculus
- Numerical Methods
- Engineering Economics
- Fluid Mechanics
- Machine Design
- Internal Combustion Engines
- Factory Organization and Management

High School 2008-2012

Bursa Işıklar Military High School - Bursa, Türkiye

PROFESSIONAL SKILLS

- Solid Edge
- Ansys Mechanical
- Catia Part design
- Matlab
- Abaqus
- ClickUp

Language

- Turkish
- English
- German

Courses

- Abaqus training
- CS50 online course
- Beckhoff PLC programming course
- Matlab training

INTERESTS



Orientering
Sailing
Cycling
Swimming



3D Printer
Board games
Electronic games



DBF 16/17 Participation
Tübitak UAV 16 participation
Tübitak UAV 17 YTU Fesa team leader
Orthosis design for a disabled dog